

SYNTHESIS AND CHARACTERIZATION OF ALUMINOBOROPHOSPHATE
COMPOUNDS BY HYDROTHERMAL AND SOLID – STATE METHODS

A THESIS SUBMITTED TO
THE GRADUATE SCHOOL OF NATURAL AND APPLIED SCIENCES
OF
THE MIDDLE EAST TECHNICAL UNIVERSITY

BY

SEHER KARABIÇAK

IN PARTIAL FULFILLMENT OF THE REQUIREMENTS FOR THE DEGREE
OF
MASTER OF SCIENCE
IN
THE DEPARTMENT OF CHEMISTRY

JANUARY 2004

Approval of Graduate School of Natural and Applied Sciences

Prof.Dr. Canan Özgen
Director

I certify this thesis satisfies all the requirements as a thesis for the degree of Master of Science

Prof.Dr. Hüseyin İşçi
Head of Department

This is to certify that we have read this thesis and that in our opinion it is fully adequate, in scope and quality, as a thesis for the degree of Master of Science.

Prof.Dr. Meral Kızılyallı
Supervisor

Examining Committee Members:

Prof.Dr. Meral Kızılyallı

Prof. Dr. Mürvet Volkan

Prof. Dr. Macit Özenbaş

Assoc.Prof.Dr. Ceyhan Kayran

Dr. Ayşen Yılmaz

ABSTRACT

SYNTHESIS AND CHARACTERIZATION OF ALUMINOBOROPHOSPHATE COMPOUNDS BY HYDROTHERMAL AND SOLID – STATE METHODS

Karabıçak, Seher

Ms., Department of Chemistry

Supervisor: Prof.Dr. Meral KIZILYALLI

January 2004, 75 pages

The hydrothermal and solid state methods were used in the synthesis of some aluminoborophosphate compounds. The products were investigated by using XRD, IR, DTA, DSC, ICP and SEM methods. The solid state reactions have been studied in the range 700 – 1200°C.

Using several hydrothermal methods a novel aluminum phosphate compound $Al_{3-x}B_xP_3O_{12}$ was synthesized. The crystal system was found to be tetragonal with $a=17.1629$ and $c = 12.6084\text{Å}$ unit cell parameters and space group is $P4_21_2$ (No:90).

In anorthite mineral ($CaAl_2Si_2O_8$) by replacing two silicon with boron and phosphorus, a boron containing anorthite with the formula of $CaAl_2BPO_8$ was prepared. The indexed data was reported for the first time in this thesis. Its crystal system was found to be monoclinic with the following unit cell parameters and β angle; $a=10.0440\text{Å}$, $b = 12.6587\text{Å}$, $c = 14.4332\text{Å}$ and $\beta = 91.55^\circ$.

In this study, $\text{AlPO}_4 \cdot x\text{H}_2\text{O}$ was also obtained by a hydrothermal method while trying to synthesize $\text{AlBP}_4\text{O}_{13}$.

All the prepared compounds have been investigated by IR spectroscopy and the assignment of the functional B-O and P-O groups were done.

Keywords: Phosphate compounds, aluminum borophosphate compounds, anorthite structure, IR and X-ray powder diffraction, hydrothermal and solid-state methods.

ÖZ

ALUMİNYUM BOROFOSFAT BİLEŞİKLERİNİN HİDROTERMAL VE KATI HAL YÖNTEMLERİYLE SENTEZLENMESİ VE KARAKTERİZASYONU

Karabıçak, Seher

Yüksek Lisans, Kimya Bölümü

Tez Yöneticisi: Prof.Dr. Meral KIZILYALLI

Ocak 2004, 75 sayfa

Bu çalışmada alüminyum borofosfat bileşiklerinin sentezi için hidrotermal ve katı hal yöntemleri kullanıldı. Elde edilen ürünler XRD, IR, DTA, DSC, ICP and SEM metodları ile incelendi. Katı hal reaksiyonları 700 – 1200°C sıcaklık aralığında çalışıldı.

Çeşitli hidrotermal yöntemleri kullanılarak $Al_{3-x}B_xP_3O_{12}$ formülünde yeni bir alüminyum fosfat bileşiği sentezlendi ve kristal yapısı tetragonal olarak bulundu. Bu bileşiğin X-ışınları deseni $a = 17.1629 \text{ \AA}$ and $c = 12.6084 \text{ \AA}$ birim hücre boyutlarıyla indekslendi. Uzay grubunun $P4_212$ (No: 90) olduğu görüldü.

$CaAl_2Si_2O_8$ formülü ile gösterilen anortit mineralinde iki silisyumun bor ve fosfor ile yer değiştirmesinden yola çıkılarak $CaAlBPO_8$ yapısında bor içeren yeni bir bileşik sentezlendi. Kristal yapısı monoklinik olarak bulundu ve $a = 10.0440 \text{ \AA}$, $b=12.6587 \text{ \AA}$, $c = 14.4332 \text{ \AA}$ and $\beta = 91.55^\circ$ birim hücre boyutlarıyla indekslendi.

Ayrıca bu çalışmada hidrotermal yöntemle $AlBP_4O_{13}$ bileşiđi elde edilmek istenirken $AlPO_4 \cdot xH_2O$ bileşiđi sentezlendi.

Sentezlenen bileşiklerin hepsi IR spektroskopisi ile incelendi ve B-O ve P-O fonksiyonel gruplarının tespiti yapıldı.

Anahtar Kelimeler: Fosfat bileşikleri, alüminyum borofosfat bileşikleri, anortit yapısı, IR ve X-ışınları toz difraksiyonu, hidrotermal ve katı hal metodları.

To my family

ACKNOWLEDGEMENTS

I would like to express my sincere appreciation to my supervisor Prof.Dr. Meral Kızılyallı for her great support, trust, encouragement, assistance and patience throughout this interesting study.

I would like to express my sincere thanks to Dr. Ayşen Yılmaz for her help and support.

I would like to thank Graduate School of Natural Applied Sciences for funding my thesis with the project number of BAP-2002-07-02-00-93, and DPT Project No:BAP-01-03-DPT-2003K-120920-09.

I also give my thanks to my lab-mates Semih Seyyidođlu, Selcan Tuncel, Mustafa Geniřel and Ebubekir řen for their help.

I am grateful to my friend Elif Kōse for her friendship.

I also wish to express my deepful thanks to my lab-mate Yasemin Ŗzdil for her warm friendship, continuous help and encouragement.

I would like to thank my friend Sevil Ŗzcan for her continous patience, psychological support and endless encouragement which I appreciate so much.

Finally, my special appreciation and gratitude is devoted to my father, my mother and my sister Bahar for their trust, patience and moral support, which makes everything possible.

TABLE OF CONTENTS

ABSTRACT.....	iii
ÖZ.....	v
ACKNOWLEDGEMENTS.....	viii
TABLE OF CONTENTS.....	ix
LIST OF TABLES.....	xii
LIST OF FIGURES.....	xiv
CHAPTER	
1. INTRODUCTION.....	1
1.1 Phosphate Chemistry.....	1
1.1.1 Classification of Phosphates.....	1
1.1.1.1 Linear Polyphosphates.....	2
1.1.1.2 Cyclophosphates.....	4
1.1.1.3 Ultraphosphates.....	5
1.1.2 Applications of Phosphates.....	6
1.2 Borophosphates.....	8
1.2.1 Aluminum Borophosphates.....	9
1.2.2 Applications of Borophosphates.....	11
1.3 Anorthite.....	11
1.3.1 Physical Characteristics of Anorthite.....	13
1.4 Hydrothermal Synthesis.....	14
1.5 Solid – State Synthesis.....	14
1.6 Purpose of the Work.....	15

2. EXPERIMENTAL TECHNIQUES.....	17
2.1 Chemical Substances.....	17
2.2 Instrumentation.....	17
2.3 Experimental Procedure.....	19
2.3.1 Hydrothermal Reactions.....	19
2.3.1.1 Hydrothermal Reactions of $\text{AlCl}_3 \cdot 6\text{H}_2\text{O}$, $\text{Na}_4\text{P}_2\text{O}_7 \cdot 10\text{H}_2\text{O}$, H_3BO_3 and HNO_3 (B4).....	19
2.3.1.2 Hydrothermal Reaction of $\text{AlCl}_3 \cdot 6\text{H}_2\text{O}$, Na_2HPO_4 , H_3BO_3 and HCl (B3).....	20
2.3.2 Solid State Reactions.....	21
2.3.2.1 Solid State Reaction of Al_2O_3 , B_2O_3 and $(\text{NH}_4)_2\text{HPO}_4$ (A1).....	21
2.3.2.2 Synthesis of Boron and Phosphorus Containing Anorthite by Solid State Reactions (A4, A5).....	21
3. RESULTS and DISCUSSION.....	24
3.1 Hydrothermal Reactions.....	24
3.1.1 Hydrothermal Reactions of $\text{AlCl}_3 \cdot 6\text{H}_2\text{O}$, $\text{Na}_4\text{P}_2\text{O}_7 \cdot 10\text{H}_2\text{O}$, H_3BO_3 and HNO_3	24
3.1.1.1 Hydrothermal Reaction with $\text{AlCl}_3 \cdot 6\text{H}_2\text{O}$, $\text{Na}_4\text{P}_2\text{O}_7 \cdot 10\text{H}_2\text{O}$, H_3BO_3 without HNO_3 (B6).....	36
3.1.1.2 Hydrothermal Reaction with $\text{AlCl}_3 \cdot 6\text{H}_2\text{O}$, $\text{Na}_4\text{P}_2\text{O}_7 \cdot 10\text{H}_2\text{O}$, HNO_3 without H_3BO_3 (B7).....	39
3.1.2 Hydrothermal Reaction of $\text{AlCl}_3 \cdot 6\text{H}_2\text{O}$, Na_2HPO_4 , H_3BO_3 and HCl (B3).....	42
3.2 Solid State Reactions.....	48
3.2.1 Solid State Reaction of Al_2O_3 , B_2O_3 and $(\text{NH}_4)_2\text{HPO}_4$ (A1).....	48
3.2.2 Synthesis of Boron and Phosphorus Containing Anorthite by Solid State Reactions (A4, A5).....	53

4. CONCLUSION.....	65
REFERENCES.....	67

APPENDIX

A. The X-ray Powder Diffraction Data of BPO_4	72
B. The X-ray Powder Diffraction Data of $\text{AlPO}_4 \cdot x\text{H}_2\text{O}$	73
C. The X-ray Powder Diffraction Data of $\text{Al}(\text{PO}_3)_3$	74
D. The X-ray Powder Diffraction Data of AlPO_4	75

LIST OF TABLES

TABLES

1.1 Silica Free Mullite Phases Revealed by Powder XRD after Crystallization.....	10
2.1 The Experimental Conditions for the Hydrothermal Reactions of $\text{AlCl}_3 \cdot 6\text{H}_2\text{O}$, $\text{Na}_4\text{P}_2\text{O}_7 \cdot 10\text{H}_2\text{O}$, H_3BO_3 and HNO_3	20
2.2 Experimental Conditions for Hydrothermal Reaction of $\text{AlCl}_3 \cdot 6\text{H}_2\text{O}$, Na_2HPO_4 , H_3BO_3 and HCl	20
2.3 Experimental Conditions for Solid State Reaction of Al_2O_3 , B_2O_3 and $(\text{NH}_4)_2\text{HPO}_4$	21
2.4 Experimental conditions for Solid State Reaction of CaCO_3 , Al_2O_3 , B_2O_3 and $(\text{NH}_4)_2\text{HPO}_4$	22
2.5 Experimental conditions for Solid State Reaction of CaO , Al_2O_3 , B_2O_3 and $(\text{NH}_4)_2\text{HPO}_4$	23
3.1 The XRD Patttern of The Products.....	24
3.2 The X-Ray Powder Diffraction Data of The Product Obtained from $\text{AlCl}_3 \cdot 6\text{H}_2\text{O} + 5 \text{HNO}_3 + 2\text{Na}_4\text{P}_2\text{O}_7 \cdot 10\text{H}_2\text{O} + \text{H}_3\text{BO}_3$ (B4, 1000°C).....	26
3.3 The X-Ray Powder Diffraction Data of The product Obtained from $\text{AlCl}_3 \cdot 6\text{H}_2\text{O} + 5 \text{HNO}_3 + 2\text{Na}_4\text{P}_2\text{O}_7 \cdot 10\text{H}_2\text{O} + \text{H}_3\text{BO}_3$ (B5, 1080°C).....	27
3.4 Assignments for The IR Spectra of The Product for Exp. No: B5 100°C and 1080°C	31
3.5 XRD Data of the Product Obtained Through Hydrothermal Reactions (without HNO_3) (B6).....	36
3.6 IR Frequencies of The product (B6 Air dried).....	37
3.7 XRD Data of the Product Obtained from $\text{AlCl}_3 \cdot 6\text{H}_2\text{O}$, $\text{Na}_4\text{P}_2\text{O}_7 \cdot 10\text{H}_2\text{O}$ and HNO_3 by Hydrothermal Reaction (B7).....	40

3.8 The X-Ray Powder Diffraction Data of the Product Obtained from $\text{AlCl}_3 \cdot 6\text{H}_2\text{O}$, Na_2HPO_4 , H_3BO_3 and HCl (B3).....	42
3.9 Assignments for the IR Spectra of the Product for Exp. No: B3.....	45
3.10 Experimental Conditions of Exp.No: A1.....	48
3.11 XRD Data of the Product Obtained by the Solid State Reactions at Different Temperatures (Exp.No. A1).....	49
3.12 IR Frequencies of The Product (A1) at 800°C and 990°C	50
3.13 The X-Ray Powder Diffraction Data of the Product Obtained from CaCO_3 , Al_2O_3 , B_2O_3 and $(\text{NH}_4)_2\text{HPO}_4$ (Exp.No: A4 1000°C).....	54
3.14 X-Ray Diffraction Data of Boron and Phosphorus Containing Anorthite, $\text{CaAl}_2\text{BPO}_8$ (sample A5 1000°C).....	58
3.15 Experimental Conditions for the Synthesis of Boron and Phosphorus Containing Anorthite.....	63
3.16 IR Frequencies of The Product Obtained from CaO , Al_2O_3 , B_2O_3 and $(\text{NH}_4)_2\text{HPO}_4$ Exp.No: A5 (1000°C).....	63

LIST OF FIGURES

FIGURES

1.1 A polyphosphate chain.....	2
1.2 A tetraphosphate group as observed in $\text{Cr}_2\text{P}_4\text{O}_{13}$	3
1.3 The $\text{P}_{12}\text{O}_{36}$ ring anion observed in $\text{Cs}_3\text{V}_3\text{P}_{12}\text{O}_{36}$	4
1.4 A discrete ultraphosphate anion, $[\text{P}_8\text{O}_{23}]^{6-}$, as observed in $\text{Fe Na}_3\text{P}_8\text{O}_{23}$	5
1.5 An infinite ultraphosphate-ribbon anion as observed in $\text{YCaP}_7\text{O}_{20}$	6
1.6 The anorthite mineral.....	12
3.1 The XRD pattern of The product Obtained from $\text{AlCl}_3.6\text{H}_2\text{O} + 5 \text{HNO}_3 + 2\text{Na}_4\text{P}_2\text{O}_7.10\text{H}_2\text{O} + \text{H}_3\text{BO}_3$ Exp.No: B4 (1000°C).....	28
3.2 The XRD pattern of The product Obtained from $\text{AlCl}_3.6\text{H}_2\text{O} + 5 \text{HNO}_3 + 2\text{Na}_4\text{P}_2\text{O}_7.10\text{H}_2\text{O} + \text{H}_3\text{BO}_3$ Exp.No: B5 (1080°C).....	29
3.3 The IR Spectra of The product Obtained from $\text{AlCl}_3.6\text{H}_2\text{O} + 5 \text{HNO}_3 + 2\text{Na}_4\text{P}_2\text{O}_7.10\text{H}_2\text{O} + \text{H}_3\text{BO}_3$ Exp.No: B4 (1000°C).....	30
3.4 The IR Spectra of The product Obtained from $\text{AlCl}_3.6\text{H}_2\text{O} + 5 \text{HNO}_3 + 2\text{Na}_4\text{P}_2\text{O}_7.10\text{H}_2\text{O} + \text{H}_3\text{BO}_3$ Exp.No: B5 (1080°C).....	32
3.5 The IR Spectra of The product Obtained from $\text{AlCl}_3.6\text{H}_2\text{O} + 5 \text{HNO}_3 + 2\text{Na}_4\text{P}_2\text{O}_7.10\text{H}_2\text{O} + \text{H}_3\text{BO}_3$ Exp.No: B5 (100°C).....	33
3.6 DTA study of Exp.No: B5 (air dried).....	34
3.7 The SEM photograph of $\text{Al}_{3-x}\text{B}_x\text{P}_3\text{O}_{12}$	35
3.8 The IR Spectra of The product Obtained from $\text{AlCl}_3.6\text{H}_2\text{O} + 2\text{Na}_4\text{P}_2\text{O}_7.10\text{H}_2\text{O} + \text{H}_3\text{BO}_3$ Exp.No: B6.....	38
3.9 DTA study of Exp.No: B6.....	39
3.10 The IR Spectra of The product Obtained from $\text{AlCl}_3.6\text{H}_2\text{O} + 5 \text{HNO}_3 + 2\text{Na}_4\text{P}_2\text{O}_7.10\text{H}_2\text{O}$ Exp.No: B7.....	41

3.11 The XRD pattern of the Product Obtained from $\text{AlCl}_3 \cdot 6\text{H}_2\text{O}$, Na_2HPO_4 , H_3BO_3 and HCl Exp.No: B3.....	44
3.12 The IR Spectra of the Product Obtained from $\text{AlCl}_3 \cdot 6\text{H}_2\text{O}$, Na_2HPO_4 , H_3BO_3 and HCl Exp.No: B3.....	46
3.13 DSC study of the Product Obtained from $\text{AlCl}_3 \cdot 6\text{H}_2\text{O}$, Na_2HPO_4 , H_3BO_3 and HCl Exp.No: B3.....	47
3.14 The XRD pattern of The Product Obtained from Al_2O_3 , B_2O_3 and $(\text{NH}_4)_2\text{HPO}_4$ Exp.No: A1.....	51
3.15 The IR Spectra of The Product Obtained from Al_2O_3 , B_2O_3 and $(\text{NH}_4)_2\text{HPO}_4$ Exp.No: A1.....	52
3.16 The XRD pattern of the Product Obtained from CaCO_3 , Al_2O_3 , B_2O_3 and $(\text{NH}_4)_2\text{HPO}_4$ Exp.No: A4.....	56
3.17 The IR Spectra of the Product Obtained from CaCO_3 , Al_2O_3 , B_2O_3 and $(\text{NH}_4)_2\text{HPO}_4$ Exp.No: A4.....	57
3.18 The XRD pattern of the Product Obtained from CaO , Al_2O_3 , B_2O_3 and $(\text{NH}_4)_2\text{HPO}_4$, Exp.No: A5.....	61
3.19 The IR Spectra of the Product Obtained from CaO , Al_2O_3 , B_2O_3 and $(\text{NH}_4)_2\text{HPO}_4$ Exp.No: A5.....	62

CHAPTER I

INTRODUCTION

1.1 Phosphate Chemistry

Three forms of phosphorus exist, white, black, and red phosphorus. Behind this very simplified scheme, reality is much more complicated. In fact, each of these three forms have several crystalline modifications and in many cases the mechanisms of transformation are complex and sometimes not reproducible [1].

1.1.1 Classification of Phosphates

Phosphates are defined as compounds which contain P-O linkages. The P-O bond has a length of 1.62 \AA , with bond angles of 130° at the O atoms and 102° at the P atoms in chain type of molecules [2]. The linear chain is illustrated in Figure 1.1. In the early nineteenth century observations showed that phosphoric acid and its salts could be transformed into various forms. This phenomena led Graham to his historic classification of phosphates into three types: orthophosphates, pyrophosphates and metaphosphates (polyphosphates) [3].

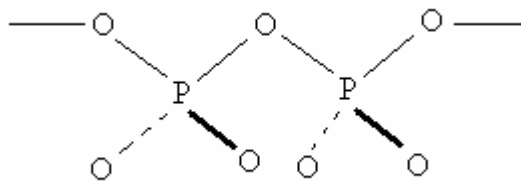


Figure 1.1 A polyphosphate chain

Orthophosphates are compounds containing discrete PO_4^{3-} ions. The pyrophosphates and metaphosphates are now known as condensed phosphates, which are formed by repeated condensation of tetrahedral $[\text{PO}_4]$ units. This results in tetrahedral chains, each sharing the O atom at one or two corners of the $[\text{PO}_4]$ tetrahedron. Diphosphate (pyrophosphate), $\text{P}_2\text{O}_7^{4-}$ is the simplest condensed phosphate anion, formed by condensation of two orthophosphate anions. The term metaphosphate refers to cyclic or chain anions which have the exact composition $(\text{PO}_3)_n^{n-}$ [3].

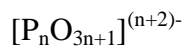
Condensed phosphates is a generic term for all phosphate polymers resulting from the elimination of water between orthophosphoric acid molecules or orthophosphate salts. Examples are linear polyphosphoric acids such as $\text{H}_4\text{P}_2\text{O}_7$, $\text{H}_5\text{P}_3\text{O}_{10}$, $\text{H}_6\text{P}_4\text{O}_{13}$ etc. with the formula $\text{H}_{n+2}\text{P}_n\text{O}_{3n+1}$ [4].

Due to their wide application, condensed phosphates were the subject of much investigation and controversy for over a century [3]. These compounds are divided into three major categories: linear polyphosphates, cyclophosphates (metaphosphates), and ultraphosphates (cages, sheets, and 3-D structures).

1.1.1.1 Linear Polyphosphates

The first type of condensation corresponds to a progressive linear linkage, by corner sharing, of PO_4 tetrahedra, this association leading to the formation of finite or

infinite chains. The corresponding phosphates are generally known as polyphosphates. The general formula for such anions is given by:



where n is the number of phosphorus atoms in the anionic entity. The first terms of this condensation, corresponding to small values of n , are commonly named oligophosphates and are well characterized up to $n = 5$. In Figure 1.2 an example of such anions is shown.

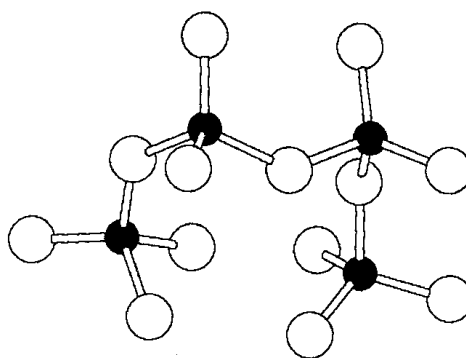


Figure 1.2 A tetrakisphosphate group as observed in $\text{Cr}_2\text{P}_4\text{O}_{13}$ by Lii et al. [5]

The terminology used for oligophosphates is well established as given below:

a) for $n = 2$, the anion is $[\text{P}_2\text{O}_7]^{4-}$ and the corresponding phosphates for a long time called pyrophosphates are now designated by the appellation of diphosphates.

b) for $n = 3$, the formula of the anion becomes $[\text{P}_3\text{O}_{10}]^{5-}$. The former appellation of tripolyphosphates for the corresponding salts is now replaced by triphosphates.

c) for $n = 4$, the anion is $[\text{P}_4\text{O}_{13}]^{6-}$ and the term tetraphosphates is now preferred the former tetrapolyphosphates.

1.1.1.2 Cyclophosphates

The second type of condensation corresponds to the formation of cyclic anions still built by a set of corner-sharing PO_4 tetrahedra leading to the following anionic formula:



These rings are well characterized for $n = 3, 4, 5, 6, 8, 9, 10$ and 12 . In Figure 1.3 a phosphoric ring anion is represented.

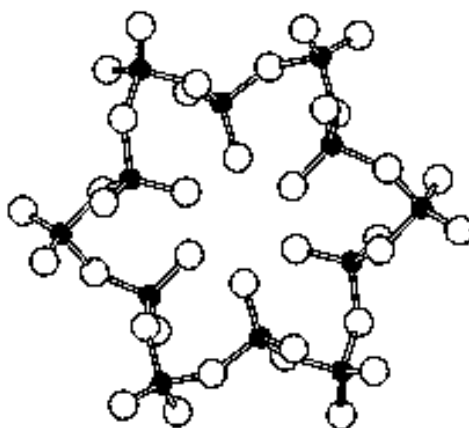
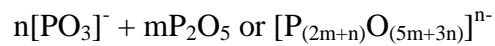


Figure 1.3 The $\text{P}_{12}\text{O}_{36}$ ring anion observed in $\text{Cs}_3\text{V}_3\text{P}_{12}\text{O}_{36}$ by Lavrov et al. [6]

1.1.1.3 Ultraphosphates

In the first two types of condensation, each PO_4 tetrahedron shares no more than two of its corners with the adjacent ones, whereas in this third type some PO_4 groups of the anionic entity share three of their corners with the adjacent ones. This type of condensation occurs in all condensed phosphates whose the anionic entities are richer in P_2O_5 than the richest members of the two classes of condensed anions, long-chain anions and ring anions. From this definition, the formulation of the anion is given by:



The corresponding salts are generally called ultraphosphates. This very general formulation corresponds to an infinite number of branches according to the values of m and n .

The ultraphosphate anions exist as finite groups like in $\text{FeNa}_3\text{P}_8\text{O}_{23}$ (Figure 1.4), as infinite ribbons like in $\text{YCaP}_7\text{O}_{20}$ (Figure 1.5), as layers of three dimensional networks [1].

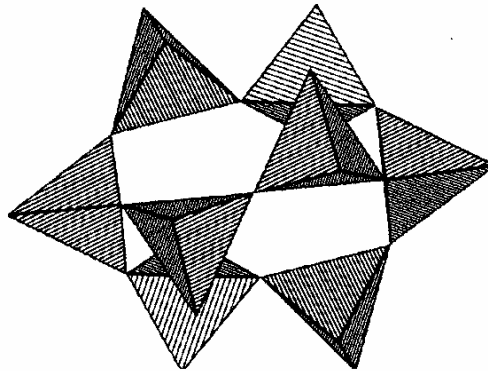


Figure 1.4 A discrete ultraphosphate anion, $[\text{P}_8\text{O}_{23}]^{6-}$, as observed in $\text{Fe Na}_3\text{P}_8\text{O}_{23}$ [7].

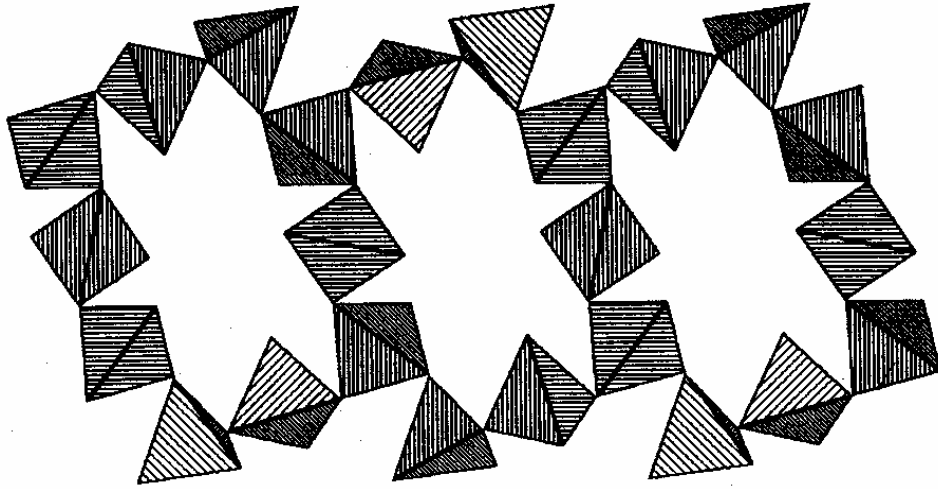


Figure 1.5 An infinite ultraphosphate-ribbon anion as observed in $YCaP_7O_{20}$ [8].

1.1.2 Applications of Phosphates

Application of phosphate amendments to soils has been identified as a potentially effective in situ remediation technology [9-12]. These amendments are available in various forms, environmental-friendly, and simple to use. Phosphate has been shown to effectively immobilize Pb from aqueous solutions as well as various contaminated soils [11,13,14], to reduce plant Pb uptake [15], and to mitigate acid mine drainage by coating the pyrite surface with $FePO_4$ which hinders sulfide oxidation, reducing the transport of heavy metals [16].

The improved machinability of $Al_2O_3/LaPO_4$ composites is very essential and important for broad engineering applications of advanced ceramics [17].

Different lanthanide phosphates are constantly subject to extensive structural and spectroscopic investigations which are motivated by their important physical properties especially aiming at their application in laser devices. Among other lanthanide

phosphates, the alkali metal lanthanide double phosphates of the type $M_3Ln(PO_4)_2$ ($M = Na, K, Rb$) have been studied by several authors [18–30].

Due to the medical importance (dental caries, bone substitutes, biomineralization, biomimetics), in vitro dissolution and crystallization of calcium phosphates have been studied a lot [31-37].

Potassium titanyl phosphate (KTP) has been shown to have superior properties for several nonlinear-optical applications and in particular, for doubling the frequency of 1064 nm radiation of Nd:YAG lasers. Its high nonlinear-optical coefficients, high optical damage threshold, wide acceptance angles, and thermally stable phase-matching properties make it suitable for this purpose. In addition to having attractive nonlinear-optical characteristics, KTP has large linear electro-optical coefficients and low dielectric constants [38], which makes it attractive for various electro-optical applications, such as modulators and Q switches. KTP also has an electro-optical waveguide modulator figure of merit that is nearly double that of any other inorganic material, this suggests that KTP is also promising for integrated-optical applications [39].

Phosphate multicomponent glasses have interesting properties (high thermal expansion coefficients, low T_g , low UV cutting edge) for technological applications [40-41]. Calcium phosphate glasses, in particular, can be biocompatible. They are more or less degradable, resulting to their low durability and used for filling bone defects or for reconstructing bony tissues, respectively [42].

The sorption of Cu^{2+} , Pb^{2+} , Ni^{2+} and Cd^{2+} (divalent metals) on the aluminum III phosphate was investigated by Naeem et al [43] concerning the removal of metal ions from waste waters.

1.2 Borophosphates

Borophosphates are intermediate compounds of the systems $M_xO_y-B_2O_3-P_2O_5-(H_2O)$ which contain complex anionic structures built of BO_4 , BO_3 and PO_4 groups and their partially protonated species, respectively. Although systematic investigations of borophosphates have been started only 5 years ago numerous borophosphates and their crystal structures have already been reported up to now. A first approach to the development of a structural chemistry is based on the linking principles of the primary building units following the general line of silicate crystal chemistry [44].

To date, several metal borophosphates have been synthesized and structurally characterized. These studies show that borophosphates have a rich structural chemistry with a large variety in their anionic $[B_xP_yO_z]^{n-}$ structural building blocks [45-46]. In particular, the use of low temperature hydrothermal techniques have resulted in borophosphates with clusters, infinite chain structures, two-dimensional layer structures as well as three-dimensional framework compounds. Thus, borophosphates show a very large variety in their basic architecture. In addition, some transition metal borate phosphates have received much interest due to their potential use in optical devices [47-48].

The structural complexity of borophosphate compounds is influenced by localized bonding arrangements of the principal components, B_2O_3 and P_2O_5 . In the structure of borate, boron atoms can form planar or pyramidal BO_3 group with 3-oxygen atoms by trigonal sp^2 bonds, or tetrahedral BO_4 group with 4-oxygen atoms by tetrahedral sp^3 bonds [49]. Besides, borate can contain not only the above two simple groups, but also many complex groups, such as the more elaborate symmetrical B_3O_6 boroxol ring [50], unsymmetrical B_3O_7 ring which containing interconnected BO_3 and BO_4 [51], and infinite chain $(BO_2)_n$ containing only threefold coordinated borons [52]. In the structure of phosphate there are mainly two kinds of groups: the relatively simple PO_4 tetrahedral group, and the complex P_2O_7 group consisting of two distorted tetrahedra PO_4 with nonlinear P-O-P bond [53]. For the borophosphate Levesseur et al.

[54] reported the existence of “BPO₇ group ” which is the basic constituent of a silica-like network where B and P are four-fold coordinated and all oxygens are bridging ones. In addition, the introduction of alkaline earth oxide may create new structural units. Therefore, the considerable variety in crystal structure of borophosphate compounds provides a great deal object for the study aiming at exploring new functional materials, especially for the nonlinear optical materials. BaBPO₅ compound was first prepared by Bauer [55], who defined their chemical formula as 2BaO.B₂O₃.P₂O₅.

Recently, there has been considerable efforts made in synthesizing novel borophosphate compounds because that BPO₄ itself is a catalyst used industrially for many reactions including hydration, dehydration, alkylation, and oligomerization [56]. The studies on the structural chemistry of the borophosphates have led to the preparation of novel compounds with a range of anionic structures, such as oligomeric units, chains, ribbons, layers, and two-dimensional (2D) frameworks [57].

Most of the borophosphates are preferably prepared by the hydrothermal method at temperatures below 200°C [58].

1.2.1 Aluminum borophosphates:

The stability of silica-free-mullite structures in the Al₂O₃-B₂O₃-P₂O₅ ternary system was investigated at T = 900-1000°C by Mazza et al [59]. Mullite is one of the most investigated ceramic compounds, for its refractory properties and specific structural nature. Mullite has a general notation [Al₂]Al_{2+2x}Si_{2-2x}O_{10-x}□_x (Hereinafter brackets indicate octahedral sites, no brackets indicate tetrahedral sites, and □ stands for a vacancy).

A monophasic mullite was obtained for the composition Al₈BPO₁₆, showing that substitution of P and B for Si is possible. Another monophasic sample was obtained in the same temperature range, with composition Al_{8.6}P_{0.4}B_{1.6}O_{16.3}. Further

preparations close to the above compositions enabled them to assess the homogeneity range for these silica-free mullites. At 1000°C it was expressed by the following notation: $\text{Al}_{8+x}\text{P}_{1-x}\text{B}_{1+x}\text{O}_{16+x/2}$ with $0 \leq x \leq 0.6 \pm 0.1$. Phases revealed by powder XRD after crystallization is given in Table 1.1.

Table 1.1 Silica Free Mullite Phases Revealed by Powder XRD after Crystallization

Composition	Cryst Temp (°C)	phase(s) at 1000°C for 20 min heating time
$\text{Al}_{10}\text{BPO}_{19}$	1000	mullite-like phase + tridymite + γ -allumina
$\text{Al}_9\text{BPO}_{17.5}$	1000	mullite-like phase + tridymite + γ -allumina
$\text{Al}_8\text{BPO}_{16}$	980	pure mullite-like phase
$\text{Al}_6\text{BPO}_{13}$	980	mullite-like phase + tridymite
$\text{Al}_4\text{BPO}_{10}$	940	Al_9B_2 + high cristobalite
Al_2BPO_7	850	Al_2B + high cristobalite

Crystal structure of aluminum catena-[monohydrogenborate-dihydrogenboratebis(monohydrogenphosphate)]monohydrate, $\text{Al}[\text{B}_2\text{P}_2\text{O}_7(\text{OH})_5] \cdot \text{H}_2\text{O}$ was found to be monoclinic with the space group C2/c. The cell parameters and β angle are the following: $a = 18.994(4)$, $b = 6.704(1)$, $c = 6.910(1)$ and $\beta = 99.03(3)^\circ$. The structure of this compound is related to the structure of $\text{Fe}[\text{B}_2\text{P}_2\text{O}_7(\text{OH})_5]$, which without consideration of the crystal water in the structure of $\text{Al}[\text{B}_2\text{P}_2\text{O}_7(\text{OH})_5] \cdot \text{H}_2\text{O}$ would be an isotype [60].

Potassium aluminum catena-(monohydrogenmonoborate)-bis(monophosphate), $\text{KAl}[\text{BP}_2\text{O}_8(\text{OH})]$ was indexed in the monoclinic system with the P21/c space group and these unitcell parameters and β angle: $a = 9.255(4)$, $b = 8.190(1)$, $c = 9.323(1)$ $\beta = 102.89(3)^\circ$ [61].

1.2.2 Applications of Borophosphates

The borophosphates is suitable for use as corrosion inhibitor, antioxidant, fireproofing agent, dispersant, and binder [62].

The considerable variety in crystal structure of borophosphate compounds provides a great deal object for the study aiming at exploring new functional materials, especially for the nonlinear optical materials [63].

The phosphor SrBPO₅: Eu²⁺ shows intense luminescence under UV and X-ray radiation and was considered to be a more favorable material as an X-ray storage phosphor than the currently used BaFBr : Eu²⁺. The Stokes shift is only about 2900 cm⁻¹ [64], indicating that the relaxation in the excited state is restricted by the host lattice [65]. It seems that these borophosphates are a new system for highly efficient luminescence. The luminescence property of Sm²⁺ in alkaline earth borophosphates (MBPO₅) was found [66].

Alkali and silver borophosphates have found application as fast ion conducting glasses [67-68] while zinc-calcium borophosphate glasses are attractive candidates for applications as low-melting glass solders or glass seals [69-70].

1.3 Anorthite (CaAl₂Si₂O₈, Calcium aluminum silicate)

In this research, anorthite related calcium alumina borophosphate was investigated so some information about anorthite was given in this section.

Anorthite is an end member and one of the rarer members of the plagioclase series. The plagioclase series comprises minerals that range in chemical composition from pure NaAlSi₃O₈, albite to pure CaAl₂Si₂O₈, anorthite. Anorthite by definition must contain no more than 10% sodium and no less than 90% calcium in the sodium/calcium

position in the crystal structure. The various plagioclase feldspars are identified from each other by gradations in index of refraction and density in the absence of chemical analysis and/or optical measurements.

All plagioclase feldspars show a type of twinning that is named after albite. Albite Law twinning produces stacks of twin layers that are typically only fractions of millimeters to several millimeters thick. These twinned layers can be seen as striation like grooves on the surface of the crystal and unlike true striations these also appear on the cleavage surfaces. The Carlsbad Law twin produces what appears to be two intergrown crystals growing in opposite directions. Two different twin laws, the Manebach and Baveno laws, produce crystals with one prominent mirror plane and penetrant angles or notches into the crystal. Although twinned crystals are common, single crystals showing a perfect twin are rare and are often collected by twin fanciers.

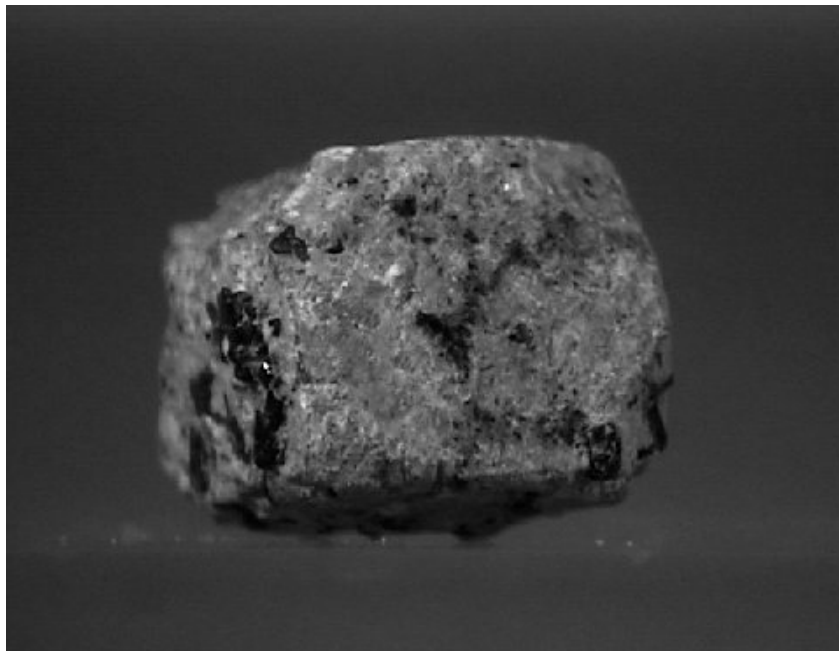


Figure 1.6 The anorthite mineral

1.3.1 Physical Characteristic of Anorthite

- **Class:** Silicates
- **Subclass:** Tectosilicates
- **Group:** Feldspars
- **Color** is usually white, gray or colorless but can be pale shades of other colors.
- **Luster** is vitreous to dull if weathered.
- **Transparency** crystals are translucent to opaque and only sometimes transparent.
- **Crystal System** is triclinic; bar 1
- **Crystal Habits** include blocky, or tabular crystals. Rarely are free crystals seen but they have a nearly rectangular or square cross-section with slanted dome and pinacoid terminations. Twinning is almost universal in all plagioclases. Crystals can be twinned according to the Albite, Carlsbad, Manebach and Baveno laws. Anorthite is usually found in contact metamorphic limestones and as a constituent in mafic igneous rocks [71].

$\text{CaAl}_2\text{Si}_2\text{O}_8$, anorthite is a triclinic crystal belonging to the plagioclase series[72]. The x-ray powder data was reported by Borg and Smith [73] with the following unit cell parameters $a = 8.1768 \text{ \AA}$, $b = 12.877 \text{ \AA}$, $c = 14.169 \text{ \AA}$, $\alpha = 93.17^\circ$, $\beta = 115.9^\circ$ and $\gamma = 91.22^\circ$ (JCPDS Card No: 20-0020 and 12-0301).

1.4 Hydrothermal Synthesis

Hydrothermal synthesis refers to the synthesis of a compound in a hydrothermal solution under the effect of temperature ($>100\text{ }^{\circ}\text{C}$) and pressures above 1 atm.

Compared with several conventional synthesis techniques, such as solid-state synthesis, sol-gel and coprecipitation methods, the hydrothermally prepared powders offer many advantages, such as high degree of crystallinity, well-controlled morphology, high purity and narrow particle size distribution [74].

Hydrothermal synthesis has been successful for the preparation of important solid state materials such as microporous and mesoporous crystals, superionic conductors, chemical sensors, electronically conducting complex oxide, complex oxide ceramics and fluorides, magnetic materials, nonlinear optical materials and luminescence phosphors [75].

This method can produce fine, high purity, stoichiometric particles of single and multicomponent metal oxides. Furthermore, if process conditions such as solution pH, solute concentration, reaction temperature, reaction time, and the type of solvent are carefully controlled, ceramic particles of the desired shape and size can be produced [76].

1.5 Solid – State Synthesis

Solid state reactions (SSRs) have been used to prepare many kinds of inorganic compounds. The SSRs applied to the preparations, however, are usually employed at elevated temperatures ($> 600\text{ K}$), because of the diffusional limitations. Recent attention of materials scientists has been focused on low temperature SSRs, because low temperatures make it possible to prepare metastable phases with interesting structures and properties [77]. Some room or low temperature SSRs have been known to occur in

systems of coordination [78] or intermetallic compounds [79] as well as soluble ionic compounds [80] (for example, $\text{KMnO}_4 + \text{MnCl}_2 \cdot 4\text{H}_2\text{O}$) with crystalline water, which affords a micro-liquid atmosphere during the reaction. In these systems considerable high mass transfer is expected because of their low melting points or low bond energies. However, no room temperature SSR, which involves some transformation of covalent networks having high bond energies and lower solubility, has been known so far. For the occurrence of the SSRs related to such transformations a high heating temperature is usually of essence [81].

The solid-state reaction technique is a convenient, inexpensive and an effective preparation method to obtain materials in high yield. Solid-state chemistry is of fundamental importance in material science [82].

1.6 Purpose of the Work

Borophosphate compounds are important as high technological materials and in the glassy form as inorganic polymers. Also, boron and phosphate materials have been widely investigated because of their potential uses. In this thesis recent literature survey has been done on physical properties of boron and phosphorus compounds since we are interested in their material properties.

In the last 10 years gadolinium tetrphosphate, $\text{Gd}_2\text{P}_4\text{O}_{13}$, has been synthesized by hydrothermal and solid-state reactions in our laboratory [83,84]. Several compounds containing $\text{P}_4\text{O}_{13}^{6-}$ anion were reported. On the other hand due to the lack of general method of preparation, tetra polyphosphates are rare and difficult to crystallize. Averbuch – Pouchot and Dunif [85] reported $\text{Pb}_3\text{P}_4\text{O}_{13}$ which is a linear polyphosphate built up by four corner sharing of PO_4 tetrahedra which has a complex triclinic structure. Bennezha et al [86] prepared $\text{Ba}_3\text{P}_4\text{O}_{13}$ from a mixture of Na_2CO_3 , BaCO_3 and $(\text{NH}_4)_2\text{HPO}_4$ (2:1:2 proportion) by fusion methods. Therefore the aim of this research is to try to synthesize new aluminum borophosphate

compounds by several hydrothermal and solid-state reactions, one of them is $\text{AlBP}_4\text{O}_{13}$, were characterised by XRD, IR, SEM, EDX and DTA methods.

In the second part of this thesis boron and phosphorus containing anorthite has been investigated.

Relation of anorthite mineral ($\text{CaAl}_2\text{Si}_2\text{O}_8$) with this research work is the close relation between silicates and borophosphates as in the case of silica free mullite ($\text{Al}_2\text{O}_3.\text{B}_2\text{O}_3.\text{P}_2\text{O}_5$). Replacement of silicon by boron and phosphorous produce interesting borophosphate compounds. In this thesis we use the term borophosphate instead of boron phosphate since we used this term in all our publications and projects. The nomenclature of boron and phosphorus compounds will be clarified and recommended in a project submitted by us to IUPAC Inorganic Chemistry Division.

CHAPTER II

EXPERIMENTAL TECHNIQUES

2.1. Chemical Substances

The following chemicals from Merck were used in the synthesis of the products: $\text{AlCl}_3 \cdot 6\text{H}_2\text{O}$, $\text{Na}_4\text{P}_2\text{O}_7 \cdot 10\text{H}_2\text{O}$, H_3BO_3 , HNO_3 , Na_2HPO_4 , HCl , Al_2O_3 , B_2O_3 , $(\text{NH}_4)_2\text{HPO}_4$, CaCO_3 and CaO .

Spectroscopic grade KBr was used for making IR pellets. It was dried 180°C for 2 hours before using.

2.2. Instrumentation

a) X-Ray Powder Diffractometer

X-ray powder diffraction patterns (XRD) were taken by using Philips diffractometer with PW 1050/25 goniometer and Co ($K\alpha$ 30-40 kV, 10-20 mA, $\lambda=1.79021\text{\AA}$) radiation and Huber Diffractometer with Cu ($K\alpha_1$ 30-40 kV, 10-20 mA, $\lambda=1.54056\text{\AA}$).

b) Infrared Spectrophotometer

Nicolet 510 FTIR Infrared Spectrometer was used in the region 400-4000 cm^{-1} . Spectra of solids were obtained from KBr pellets using KBr:Sample ratio=100mg:3mg.

c) Differential Thermal Analyzer (DTA)

Thermal behaviour of specimens was examined by Dupont thermal analyst 2000 DSC 910S model differential scanning calorimeter. About 5 mg of the specimens was inserted to the instrument and heated by 10 $^{\circ}\text{C}/\text{min}$.

d) Inductively Coupled Plasma Emission Spectroscopy

Inductively Coupled Plasma (ICP, Leeman Lab. Inc., DRE Direct reading Echelle) was used for the analysis of boron.

e) Scanning Electron Microscope (SEM)

Electron microscopy is an extremely versatile technique capable of providing structural information over a wide range of magnification. Crystals were photographed with Jeol Scanning Microscope 6400 (JSM- 6400) and the quantitative analysis of Fe, P have been done with Energy Dispersive X-ray Analyzer (EDX) (20 kV).

f) Furnaces

The solid state reactions have been carried out in air with the aid of Heraeus (KR-170), SFL West-6100 and Neyo 2-525 (computer controlled) furnaces. Heating

ranges were 550-1200 °C, 300-1200 °C and 300-900 °C respectively using Cr-Ni-Cr and Rh-Pt-Rh thermocouples. To avoid melting, reactions started at room temperature.

2.3 Experimental Procedure

2.3.1 Hydrothermal Reactions

In all hydrothermal reactions, the following chemical procedures were applied. Calculated amount of chemicals were dissolved with water and then a suitable acid mixture was added in order to dissolve the solid mixture completely in a minimum amount of solution (about 17ml). When the solution was clear enough it was poured into a Teflon autoclave and heated at 180°C in an oven for 5-12 days. After the heating process, the autoclave was taken from the oven and opened at room temperature. In order to take its solid part, it was filtered and washed with distilled water. The precipitate dried in air firstly and then heated in the oven at different temperatures. After the drying process, X-ray diffraction pattern and infrared spectrum of the sample was recorded. Then if it is found to be necessary its SEM photograph and DTA analysis has been done.

2.3.1.1 Hydrothermal Reactions of $\text{AlCl}_3 \cdot 6\text{H}_2\text{O}$, $\text{Na}_4\text{P}_2\text{O}_7 \cdot 10\text{H}_2\text{O}$, H_3BO_3 and HNO_3 (B4)

For the attempted synthesis of $\text{AlBP}_4\text{O}_{13}$ compound, through hydrothermal reactions the procedure given below has been used.

This experiment was also repeated to check the reproducibility (B5). The experimental conditions of $\text{AlCl}_3 \cdot 6\text{H}_2\text{O}$, $\text{Na}_4\text{P}_2\text{O}_7 \cdot 10\text{H}_2\text{O}$, H_3BO_3 and HNO_3 is summarized in Table 2.1. Each reaction is characterised by an experiment number which is given with the text as Exp.No.

Table 2.1 The Experimental Conditions for the Hydrothermal Reactions of $\text{AlCl}_3 \cdot 6\text{H}_2\text{O}$, $\text{Na}_4\text{P}_2\text{O}_7 \cdot 10\text{H}_2\text{O}$, H_3BO_3 and HNO_3

Exp.No	Composition				Duration (day)
	$\text{AlCl}_3 \cdot 6\text{H}_2\text{O}$	$\text{Na}_4\text{P}_2\text{O}_7 \cdot 10\text{H}_2\text{O}$	H_3BO_3	HNO_3	
B4	0.653g	2.409g	0.168g	0.9ml	9
B5	0.653g	2.409g	0.169g	0.9ml	12
B6	0.652g	2.408g	0.169g	–	7
B7	0.652g	2.409g	–	0.9ml	5

Hydrothermal reactions of $\text{AlCl}_3 \cdot 6\text{H}_2\text{O}$, $\text{Na}_4\text{P}_2\text{O}_7 \cdot 10\text{H}_2\text{O}$, H_3BO_3 and HNO_3 were tried

- a) without using HNO_3 and
- b) without using H_3BO_3 under the same conditions for comparison purposes.

2.3.1.2 Hydrothermal Reaction of $\text{AlCl}_3 \cdot 6\text{H}_2\text{O}$, Na_2HPO_4 , H_3BO_3 and HCl (B3)

In this experiment, $\text{AlCl}_3 \cdot 6\text{H}_2\text{O}$, Na_2HPO_4 , H_3BO_3 and HCl were used as the reactants. Experimental conditions for this hydrothermal reaction is given in Table 2.2.

Table 2.2 Experimental Conditions for Hydrothermal Reaction of $\text{AlCl}_3 \cdot 6\text{H}_2\text{O}$, Na_2HPO_4 , H_3BO_3 and HCl

Exp.No	Composition				Duration (day)
	$\text{AlCl}_3 \cdot 6\text{H}_2\text{O}$	Na_2HPO_4	H_3BO_3	HCl	
B3	0.979g	2.305g	0.251g	1ml	6

2.3.2 Solid State Reactions

Using different solid-state reactions the several compounds were synthesized at different temperatures and have been investigated to identify the obtained products.

2.3.2.1 Solid State Reaction of Al₂O₃, B₂O₃ and (NH₄)₂HPO₄ (A1)

The reactants were mixed in stoichiometric proportion given below in an agate mortar and the mixtures were heated with 2K/min heating rate at different temperatures in the range of 800-1140 °C given in Table 2.3. the expected reaction is

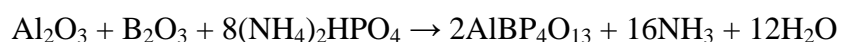


Table 2.3 Experimental Conditions for Solid State Reaction of Al₂O₃, B₂O₃ and (NH₄)₂HPO₄

Exp.No	Temperature (°C)	Time (h)
A1	800	8
A1	900	22
A1	990	15
A1	1140	10

2.3.2.2 Synthesis of Boron and Phosphorus Containing Anorthite by Solid State Reactions (A4, A5)

Boron and phosphorus containing anorthite, CaAl₂BPO₈, was predicted by changing two Si atoms with B and P in anorthite (CaAl₂Si₂O₈). The synthesis of CaAl₂BPO₈ was tried with two different procedures. In each case at least one of the reactants was different.

a) In the first procedure, the compound was synthesized by heating the stoichiometric mixture given by the following equation (Exp.No: A4). The expected reaction is the following:



Experimental conditions is given in the Table 2.4.

Table 2.4 Experimental conditions for Solid State Reaction of CaCO_3 , Al_2O_3 , B_2O_3 and $(\text{NH}_4)_2\text{HPO}_4$

Exp.No	Temperature (°C)	Time (h)
A4	700	8
A4	800	12
A4	900	11
A4	1000	14
A4	1200	5

b) In the second method, instead of CaCO_3 , CaO was used. The following reaction is expected:



Experimental conditions is given in the Table 2.5.

Table 2.5 Experimental conditions for Solid State Reaction of CaO, Al₂O₃, B₂O₃ and (NH₄)₂HPO₄

Exp.No	Temperature (° C)	Time (h)
A5	700	8
A5	800	12
A5	900	11
A5	1000	14
A5	1200	5

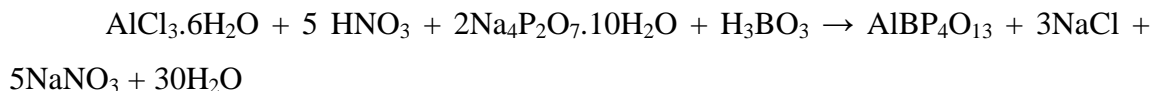
CHAPTER III

RESULTS and DISCUSSION

3.1 Hydrothermal Reactions

3.1.1 Hydrothermal Reactions of $\text{AlCl}_3 \cdot 6\text{H}_2\text{O}$, $\text{Na}_4\text{P}_2\text{O}_7 \cdot 10\text{H}_2\text{O}$, H_3BO_3 and HNO_3 (B4)

The conditions were given in page 20 in the experimental section before. The following reaction was predicted:



Since the product obtained from Exp.No: B4 is heated at 100°C , the reaction was repeated to investigate the air dried product (B5).

Table 3.1 shows the XRD pattern of the products obtained through hydrothermal reactions and heated at different temperatures.

Table 3.1 The XRD Pattern of the Products

B4 (100 C)		B4 (1000 C)		B5 (air dried)		B5 (100 C)		B5 (1080 C)	
I/I ₀	d	I/I ₀	d	I/I ₀	d	I/I ₀	d	I/I ₀	d
1	8.5633	1	8.5775	3	8.6350	3	8.4928	1	8.5633
1	4.9467	1	4.9567	–	–	–	–	–	–

Table 3.1 Continued

100	4.2876	100	4.2876	100	4.3052	100	4.3052	91	4.3052
–	–	21	4.0794	–	–	–	–	100	4.0873
1	4.0095	5	3.9866	10	4.0094	5	3.9942	7	3.9942
–	–	5	3.8183	–	–	–	–	5	3.7525
–	–	–	–	–	–	–	–	5	3.5570
–	–	–	–	–	3.6500	–	–	–	–
–	–	–	–	–	–	–	–	5	3.4811
14	3.3814	7	3.3760	100	3.3922	5	3.3922	14	3.3814
–	–	3	3.1609	–	–	–	–	12	3.1703
–	–	3	2.8735	–	–	–	–	13	2.8773
–	–	–	–	–	–	–	–	14	2.5063
11	2.4752	25	2.4752	10	2.4752	–	–	8	2.4752
–	–	–	–	3	2.2561	–	–	–	–
40	2.1421	65	2.1421	100	2.1462	100	2.1421	29	2.1421
–	–	–	–	–	–	–	–	3	2.0382
1	1.9956	1	1.9991	20	1.9973	10	1.9939	6	1.9921
–	–	1	1.9516	–	–	–	–	–	–
–	–	1	1.8850	–	–	–	–	–	–
1	1.8348	–	–	–	1.8291	–	–	–	–

The examination of the table shows that all the patterns were similar except the product dried in air and 100°C where $d = 4.08$ is missing. On the other hand presence of BPO_4 in the product (3.65, 2.25, 1.83) and disappearance after heating at 1080°C proved that B is in the solid.

The product which was heated at 1000°C (B4) and 1080°C (B5) for 6 hours were indexed in tetragonal system with the unit cell parameters of $a = 17.1629$ and $c = 12.6084$. The space group was found to be $P4_21_2$ (No:90). The space group conditions

are : hkl: no condition, ool: no condition and hoo: 2n. The indexed data is given in Table 3.2 and Table 3.3 for the products heated at 1000°C and 1080°C. Both patterns are about the same with few exceptions.

Table 3.2 The X-Ray Powder Diffraction Data of The Product Obtained from $\text{AlCl}_3 \cdot 6\text{H}_2\text{O} + 5 \text{HNO}_3 + 2\text{Na}_4\text{P}_2\text{O}_7 \cdot 10\text{H}_2\text{O} + \text{H}_3\text{BO}_3$ (Exp.No: B4 (1000°C))

I/I_0	d_{obs}	$\sin^2\theta_{\text{obs}}$	$\sin^2\theta_{\text{cal}}$	hkl
4	8.5775	0.01089	0.01088	200
2	4.9547	0.03264	0.03224	311
100	4.2876	0.04358	0.04352	400
24	4.0794	0.04815	0.04862	401
5	3.9866	0.05041	0.05080	113
4	3.8483	0.05410	0.05440	420
8	3.3760	0.07007	0.06984	303
4	3.1609	0.08019	0.08064	004
2	3.0509	0.08608	0.08608	114
4	2.8735	0.09792	0.09753	531
5	2.5034	0.12784	0.12789	631
32	2.4752	0.13077	0.13040	622, 444
68	2.1421	0.17461	0.17496	335
2	1.9991	0.20049	0.20088	661

Table 3.3 The X-Ray Powder Diffraction Data of The product Obtained from $\text{AlCl}_3 \cdot 6\text{H}_2\text{O} + 5 \text{HNO}_3 + 2\text{Na}_4\text{P}_2\text{O}_7 \cdot 10\text{H}_2\text{O} + \text{H}_3\text{BO}_3$ (Exp.No: B5 (1080°C))

I/I_0	d_{obs}	$\sin^2\theta_{\text{obs}}$	$\sin^2\theta_{\text{cal}}$	hkl
5	8.5633	0.01093	0.01088	200
91	4.3052	0.04323	0.04352	400
100	4.0873	0.04796	0.04856	401
7	3.9942	0.05022	0.05080	113
5	3.7525	0.05690	0.05624	203
5	3.5570	0.06333	0.06368	402
5	3.4811	0.06612	0.0664	412
14	3.3814	0.07007	0.06984	303
12	3.1703	0.07972	0.07888 0.08064	520 004
13	2.8773	0.09704	0.09752	531
14	2.5063	0.12755	0.12872	105
8	2.4752	0.13077	0.13144	444
29	2.1421	0.17461	0.17496	335
3	2.0382	0.19286	0.019216	544
6	1.9921	0.20189	0.20488	525

The XRD pattern of the products obtained through experiment B4 (1000°C), experiment B5 (1080°C) were given in Figure 3.1 and Figure 3.2.

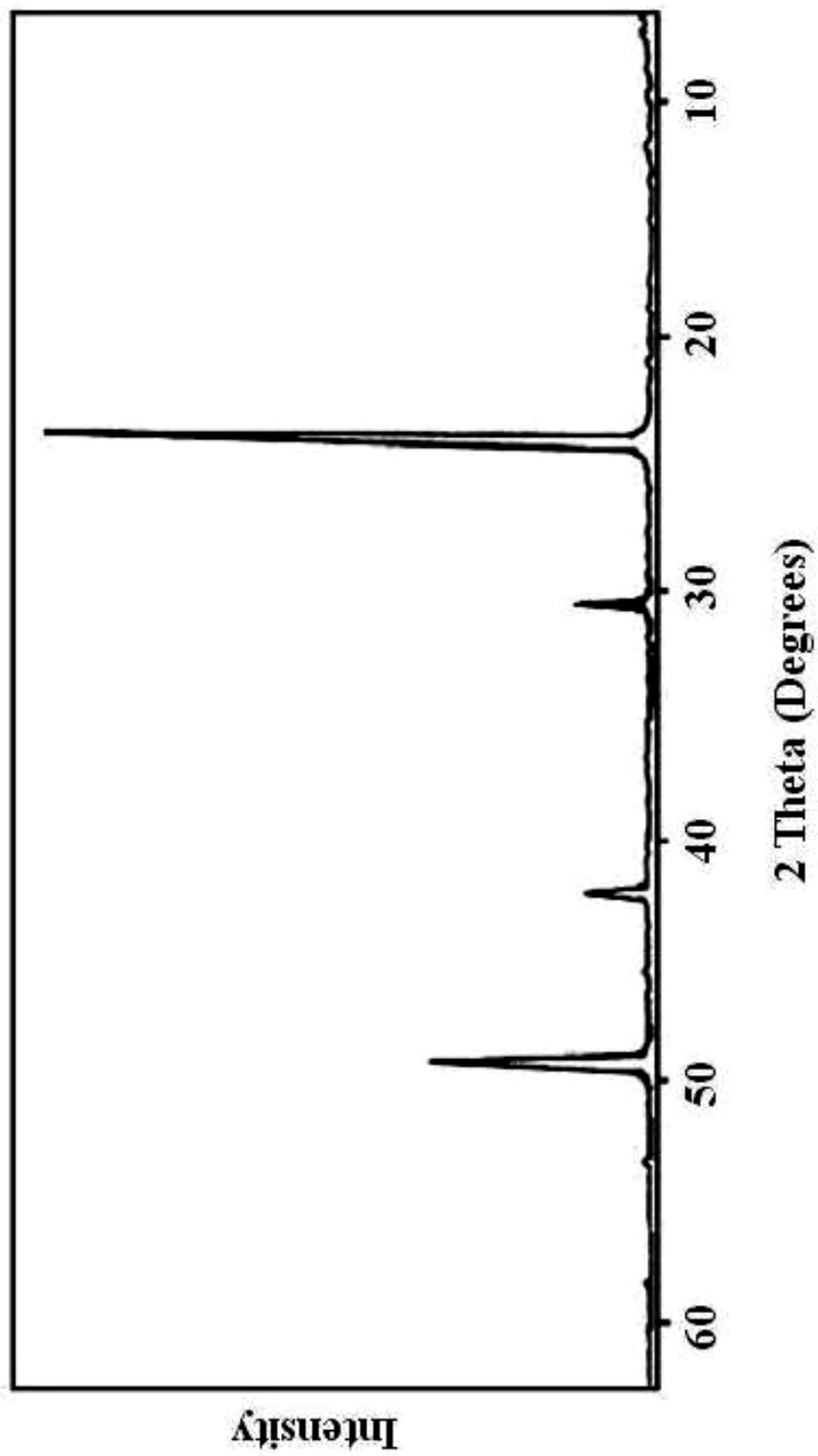


Figure 3.1. The XRD pattern of The product Obtained from $\text{AlCl}_3 \cdot 6\text{H}_2\text{O} + 5 \text{HNO}_3 + 2\text{Na}_4\text{P}_2\text{O}_7 \cdot 10\text{H}_2\text{O} + \text{H}_3\text{BO}_3$ Exp.No: B4 (1000°C)

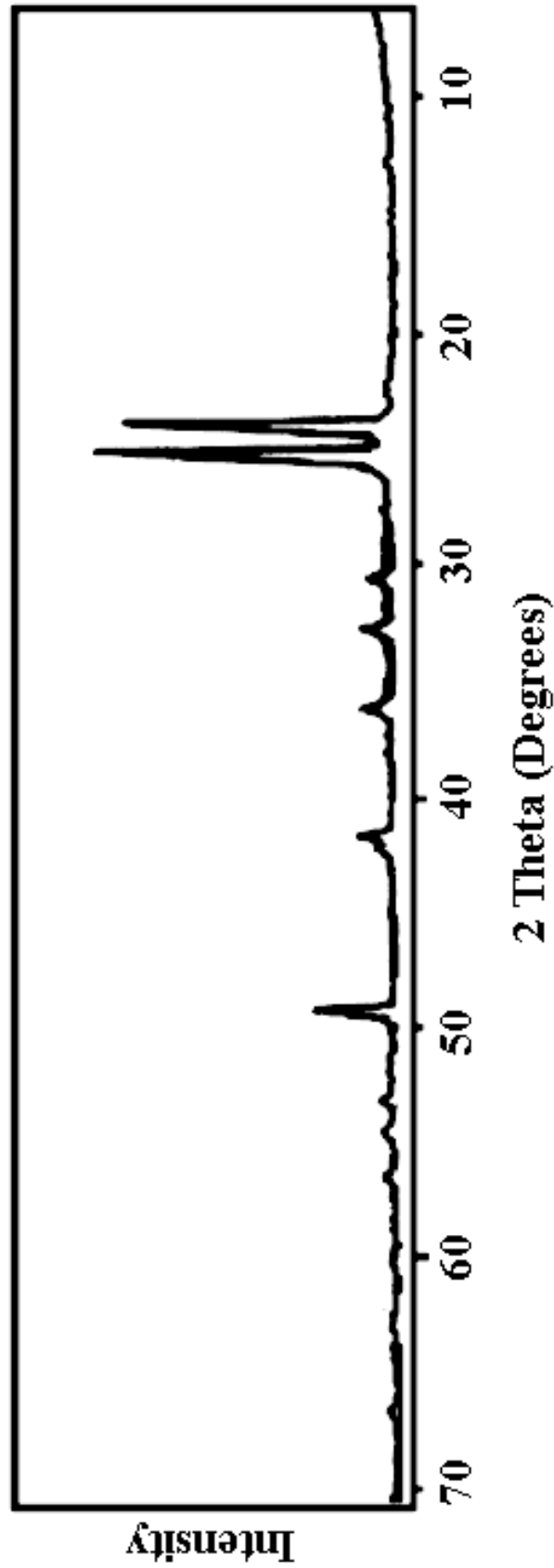


Figure 3.2 The XRD pattern of The product Obtained from $\text{AlCl}_3 \cdot 6\text{H}_2\text{O} + 5 \text{HNO}_3 + 2\text{Na}_4\text{P}_2\text{O}_7 \cdot 10\text{H}_2\text{O} + \text{H}_3\text{BO}_3$ Exp.No: B5 (1080°C)

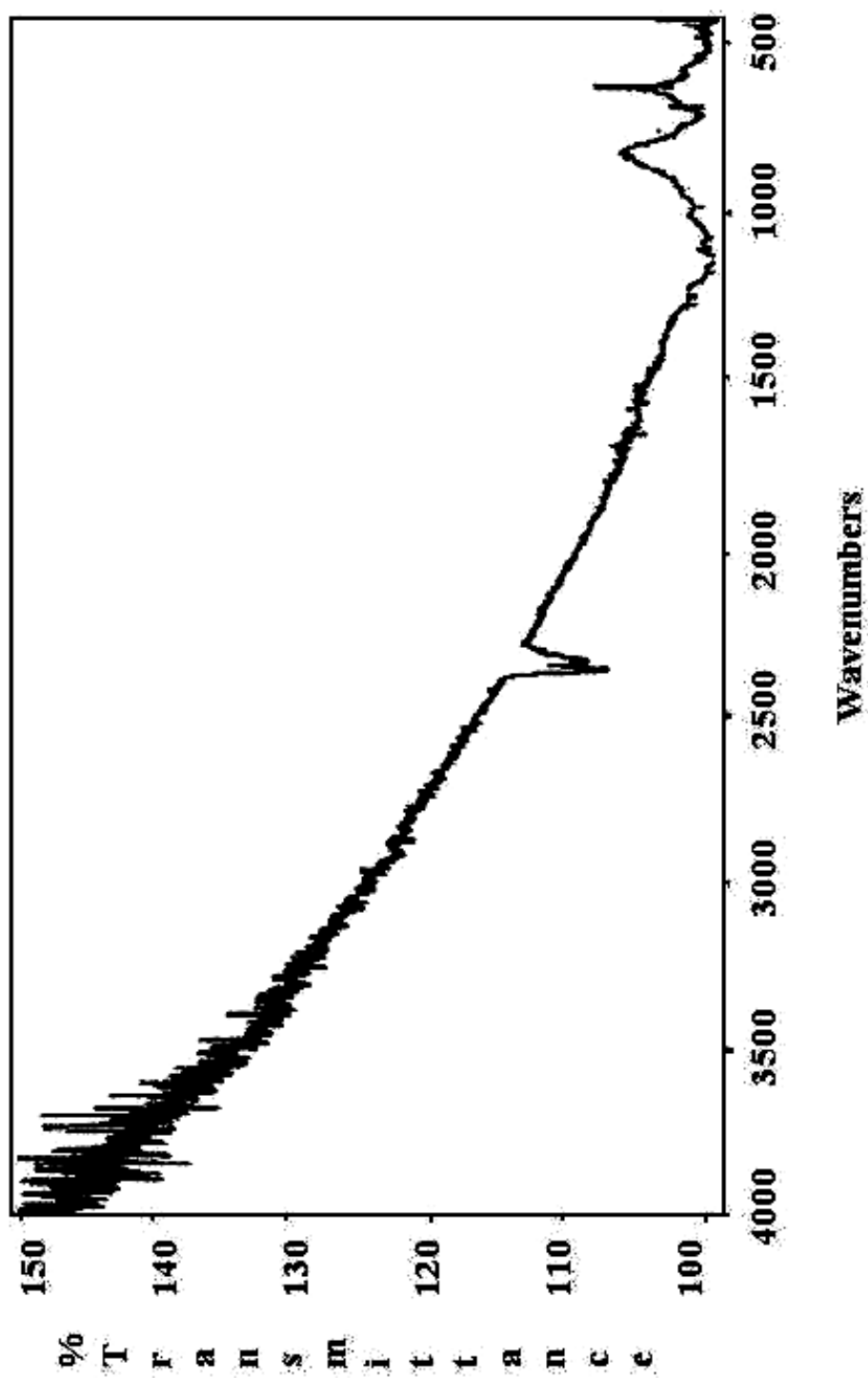


Figure 3.3 The IR Spectra of The product Obtained from $\text{AlCl}_3 \cdot 6\text{H}_2\text{O} + 5 \text{HNO}_3 + 2\text{Na}_4\text{P}_2\text{O}_7 \cdot 10\text{H}_2\text{O} + \text{H}_3\text{BO}_3$ Exp.No: B4 (1000°C)

The IR data of the air dried product is very complex and assignments to the frequencies were very difficult. IR spectrum of the product at 100°C (B5) and 1080°C (B5) were given in Figure 3.4 and Figure 3.5.

Table 3.4 Assignments for The IR Spectra of The Product for Exp. No: B5 100°C and 1080°C

B5 (100°C)		B5 (1080°C)	
Frequency (cm⁻¹)	Assignment	Frequency (cm⁻¹)	Assignment
3440	OH stretching in H ₂ O	–	–
1630	OH deformation in H ₂ O	–	–
1117	ν_3 PO ₄	1117	ν_3 PO ₄
1080	ν_3 PO ₄ , ν_3 BO ₄	–	–
1040	ν_3 PO ₄ , ν_3 BO ₄	1022	ν_3 PO ₄ , ν_3 BO ₄
970	ν_1 PO ₄	–	–
703	P-O-P, B-O-P	703, 710	B-O-P
650	ν_4 PO ₄	640, 624	ν_4 PO ₄
–	–	568	ν_4 PO ₄ , ν_4 BO ₄
–	–	488	ν_2 PO ₄ , ν_2 BO ₄
433, 437, 401	ν_2 PO ₄	430	ν_2 PO ₄ , ν_2 BO ₄

The IR data for the product obtained at 1080°C fits the data for a tetragonal structure. The 100°C product contains water and the X-Ray data could not be indexed

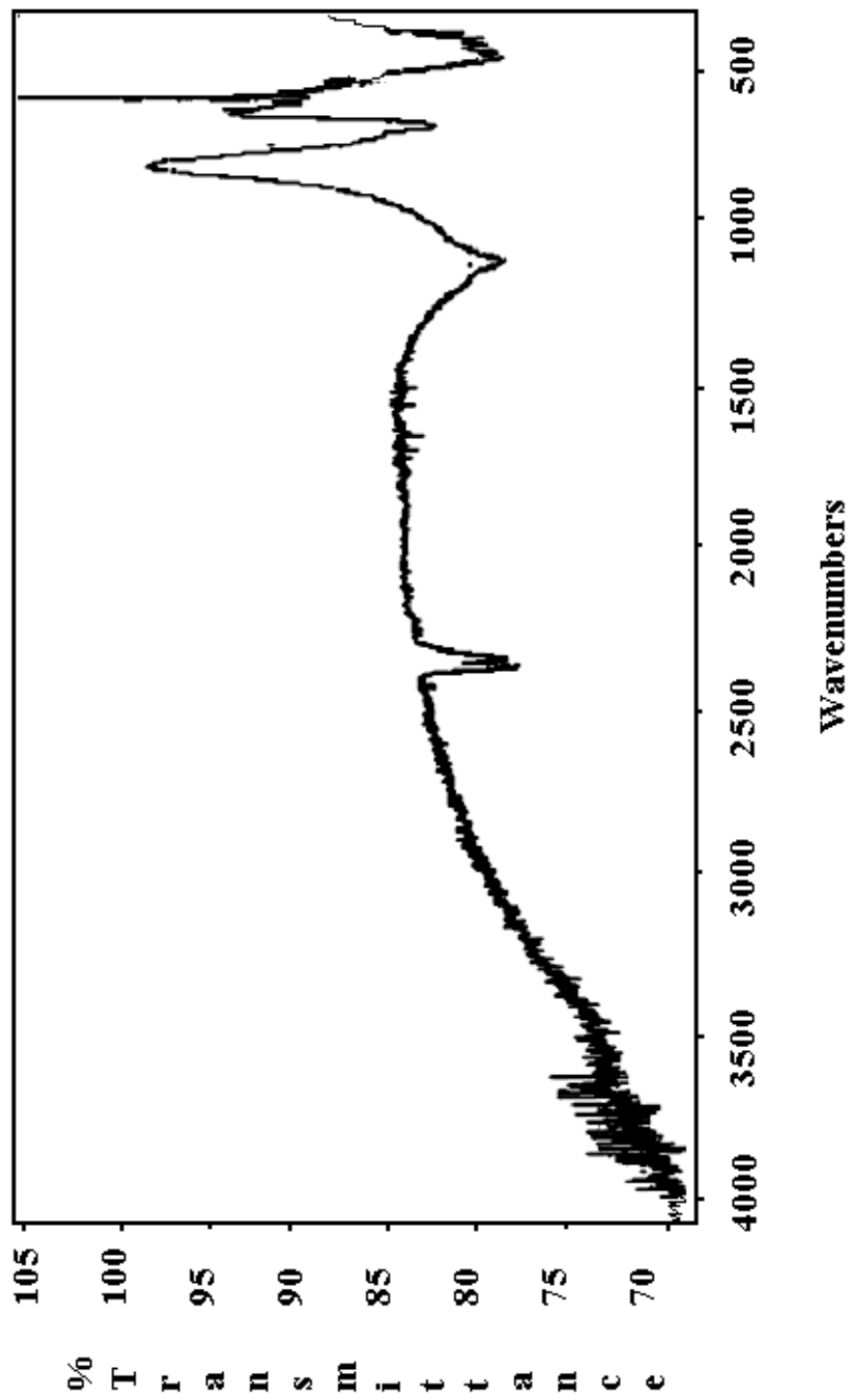


Figure 3.4 The IR Spectra of The product Obtained from $\text{AlCl}_3 \cdot 6\text{H}_2\text{O} + 5 \text{HNO}_3 + 2\text{Na}_4\text{P}_2\text{O}_7 \cdot 10\text{H}_2\text{O} + \text{H}_3\text{BO}_3$ Exp.No: B5 (1080°C)

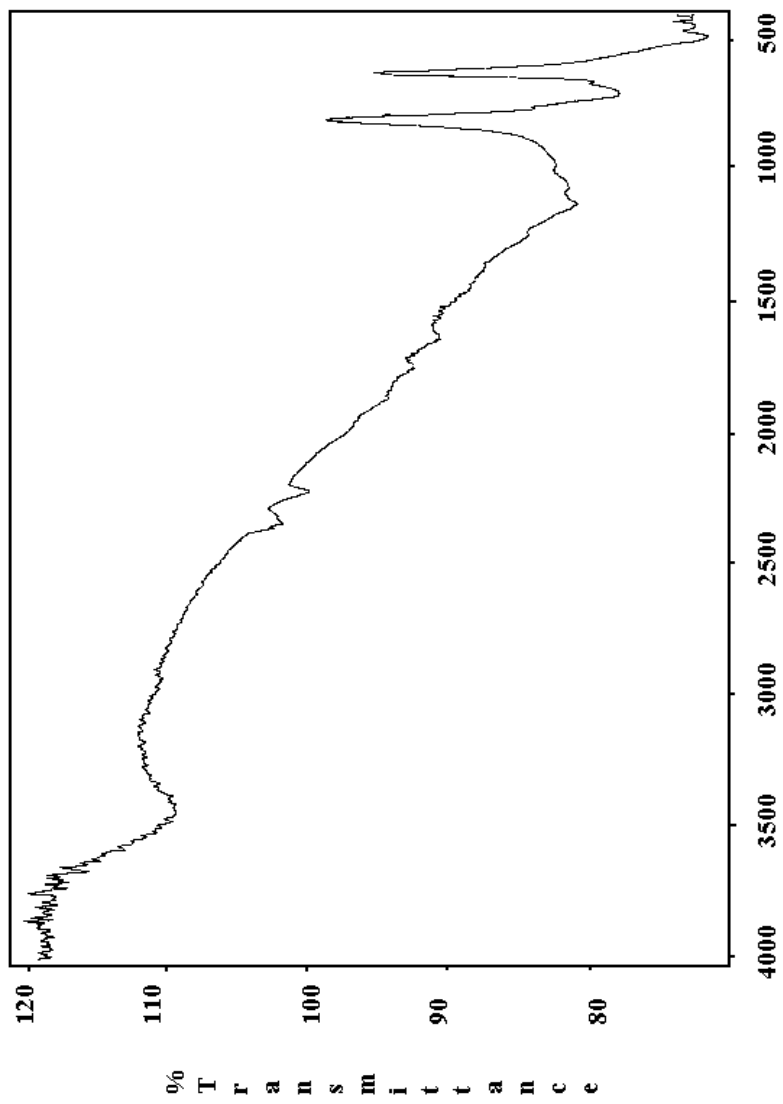


Figure 3.5 The IR Spectra of The product Obtained from $\text{AlCl}_3 \cdot 6\text{H}_2\text{O} + 5 \text{HNO}_3 + 2\text{Na}_4\text{P}_2\text{O}_7 \cdot 10\text{H}_2\text{O} + \text{H}_3\text{BO}_3$ Exp.No: B5 (100°C)

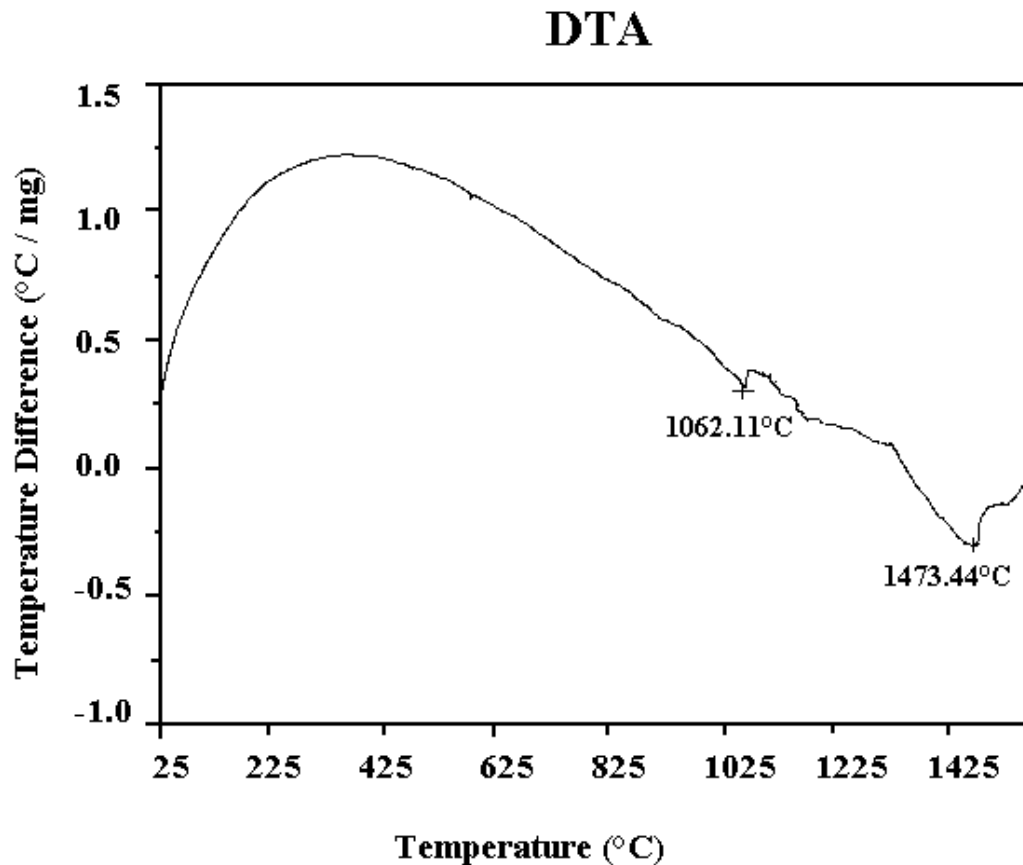


Figure 3.6 DTA study of Exp.No: B5 (air dried)

Figure 3.6 shows the DTA data of the product obtained at 100°C. The peak at 1062°C could be due to formation of the indexed crystal structure given in Table 3.3. This is the reason that we heated the product at 1080°C. 1473,44°C may corresponds to glass transition temperature.

The EDX analysis for B5 1080°C gave on Al:P molar ratio as 2:3 so the predicted product $\text{AlBP}_4\text{O}_{13}$ was not obtained.

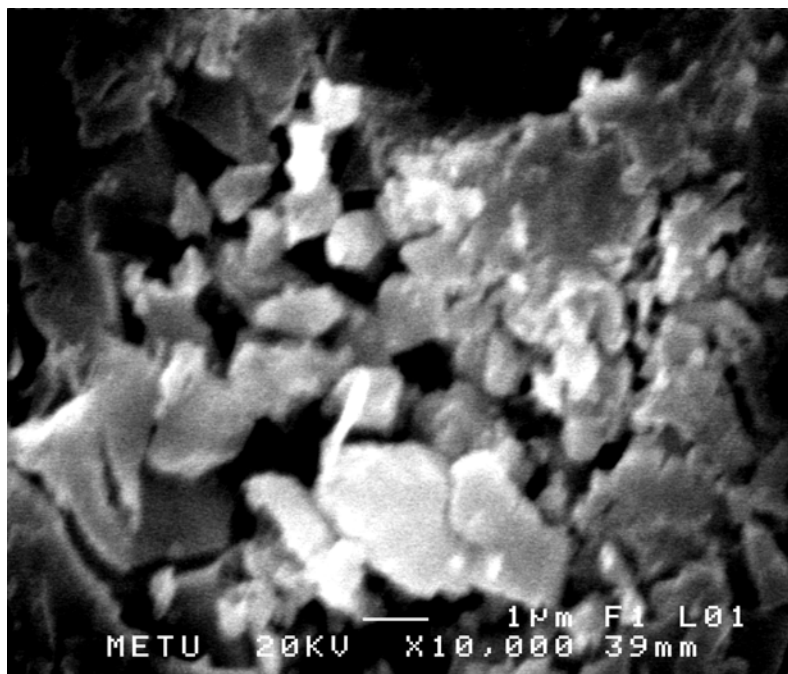
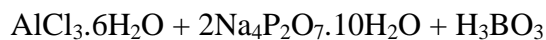


Figure 3.7 The SEM photograph of $\text{Al}_{3-x}\text{B}_x\text{P}_3\text{O}_{12}$

The SEM photograph (Figure 3.7) shows particles of irregular shape and size. In the IR spectra the presence of P-O symmetric and asymmetric stretching vibrations due to PO_4 and BO_4 ion and B-O-P modes revealed that the compound could be $\text{Al}_2\text{BP}_3\text{O}_{12}$. Bands due to $\text{P}_4\text{O}_{13}^-$ was not present [83]. But ICP analysis of the compound showed trace amount of boron. This could be due to insoluble compound and high amount of dilution so that B can not be detected. Anyway instead of $\text{Al}_3\text{P}_3\text{O}_{12}$, $\text{Al}_{3-x}\text{B}_x\text{P}_3\text{O}_{12}$ is reasonable since B is present in the compound. Another proof of the presence of B in the product is the analysis of solution after separating the solid product. After filtering the solution was dried at 180°C for 2-3 days. In the IR data, modes due to B-O are not present, most of the frequencies belong to NO_3^- . If B is not present in the product than the formula ends up to be $\text{Al}_3\text{P}_3\text{O}_{12}$ (AlPO_4) so bands due to B-O and B-O-P vibrations should not be present in the pattern. In this case the formula can be written as $\text{Al}_{3-x}\text{B}_x\text{P}_3\text{O}_{12}$ where B is in the solid solution.

3.1.1.1 Hydrothermal Reaction with $\text{AlCl}_3 \cdot 6\text{H}_2\text{O}$, $\text{Na}_4\text{P}_2\text{O}_7 \cdot 10\text{H}_2\text{O}$ and H_3BO_3 without HNO_3 (B6)

The following stoichiometric mixture was used in the hydrothermal reaction without using HNO_3 under the same conditions as discussed in experimental section.



The procedure and the amounts are the same as B4 and B5 experiments given on page 20. Only HNO_3 was not added to the solution. The obtained white powder dried in air and subjected to XRD and IR examination.

In the Table 3.5 the X-Ray diffraction data of the obtained product is given.

Table 3.5 XRD Data of the Product Obtained Through Hydrothermal Reactions (without HNO_3)

I/I_0	d_{obs}	I/I_0	d_{obs}
10	7.6155	3	2.5709
5	6.9968	4	2.4697
8	4.8210	2	2.4262
2	4.5982	3	2.3003
3	3.6871	1	2.1668
3	3.4926	1	2.1140
2	3.3922	1	2.0647
4	3.1792	1	1.9582
3	3.1332	3	1.8911
4	3.0313	1	1.7584
3	2.7286	1	1.7532
2	2.6813	2	1.5684

In the IR data (Figure 3.8 and Table 3.6) the following frequencies were obtained.

Table 3.6 IR Frequencies of the product (B6 Airdried)

Frequency (cm ⁻¹)	Assignment
3590	OH ⁻ in hydroxides
1219	ν_{as} PO ₂
1160	ν (P=O), ν_s PO ₂
1081	ν_3 PO ₄
1026	ν_3 PO ₄
923	ν_1 PO ₄
768	P-O-P in polyphosphate
668	ν_4 PO ₄ , δ PO ₂
547	ν_4 PO ₄ , δ PO ₂
486	ν_2 PO ₄ , δ PO ₂
446	ν_2 PO ₄
420	ν_2 PO ₄

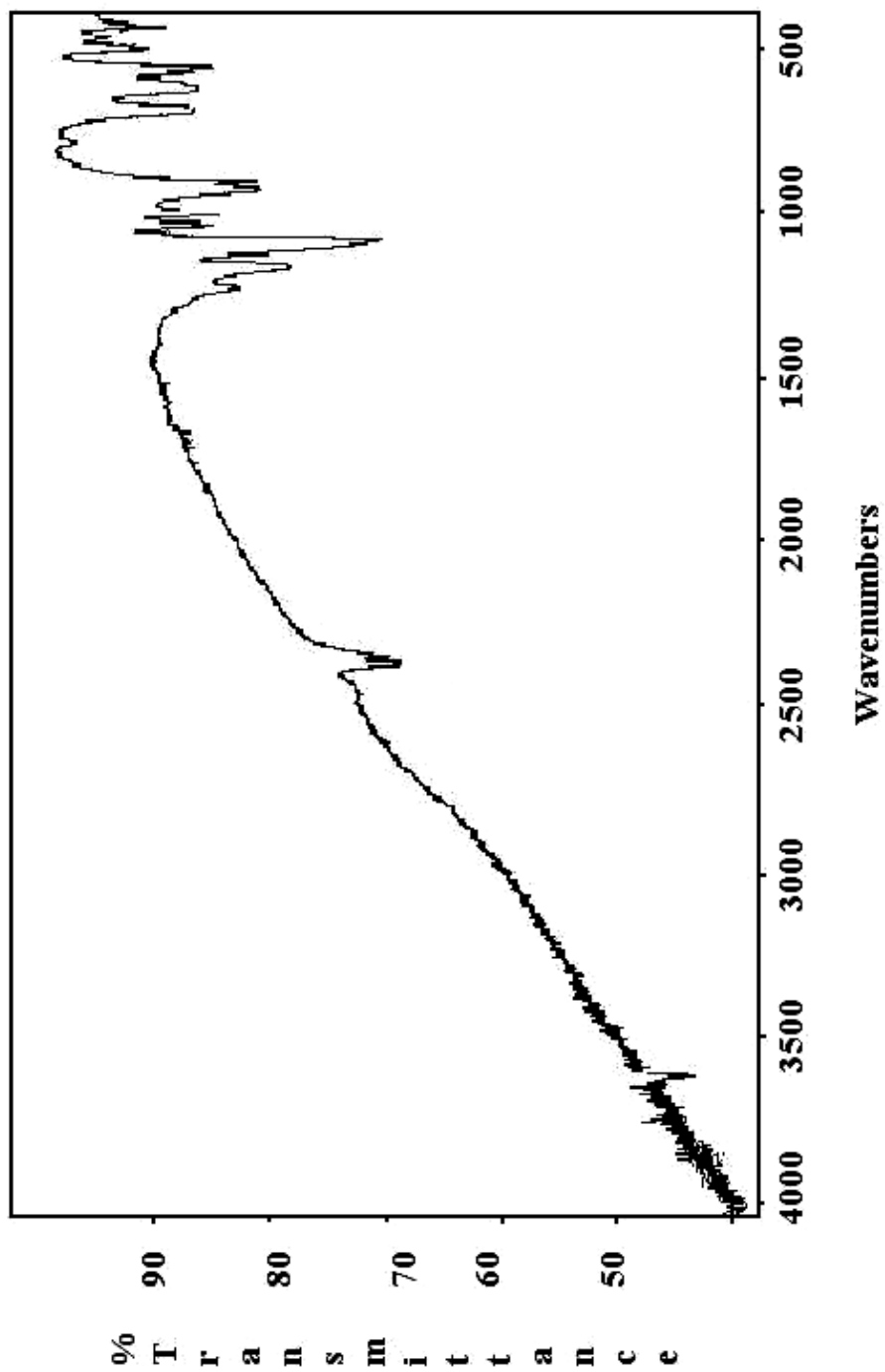


Figure 3.8 The IR Spectra of The product Obtained from $\text{AlCl}_3 \cdot 6\text{H}_2\text{O}$
 $+ 2\text{Na}_4\text{P}_2\text{O}_7 \cdot 10\text{H}_2\text{O} + \text{H}_3\text{BO}_3$ Exp.No: B6

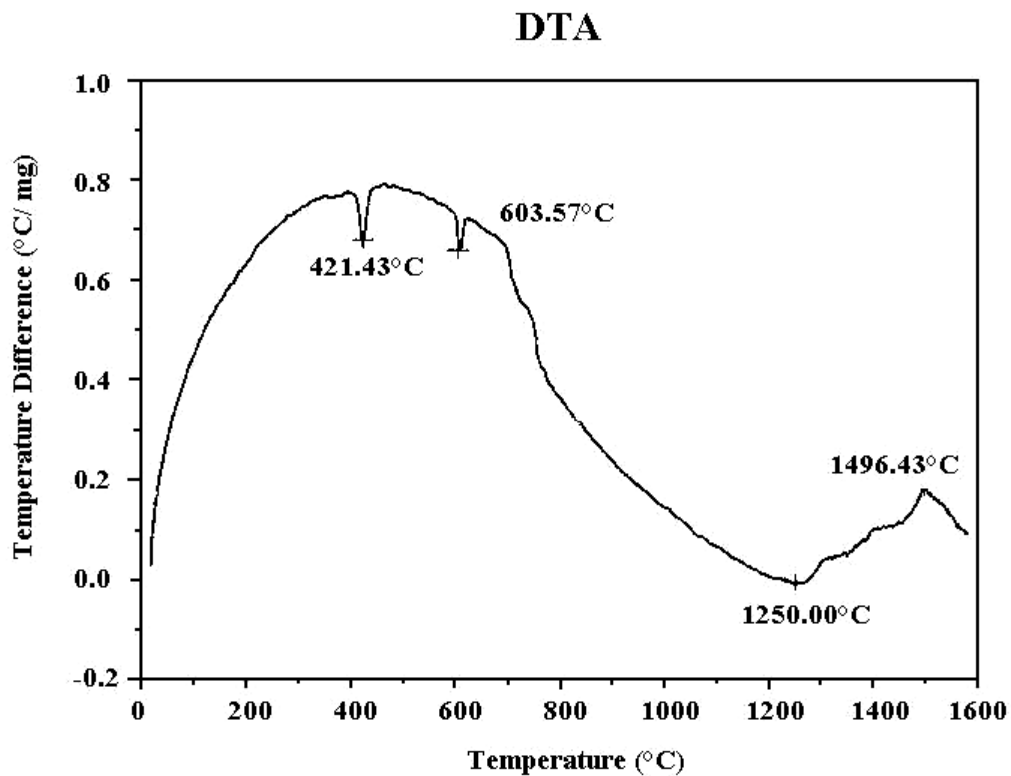


Figure 3.9 DTA study of Exp.No: B6

The product could not be identified. The DTA analysis show 3 peaks at 425, 600 and 1250 °C so the product heated at these temperatures subjected to IR analysis. The IR obtained showed gradual change from polyphosphates to orthophosphates at these temperatures. The identification of the product and IR assignments needs further investigation.

3.1.1.2 Hydrothermal Reaction with $\text{AlCl}_3 \cdot 6\text{H}_2\text{O}$, $\text{Na}_4\text{P}_2\text{O}_7 \cdot 10\text{H}_2\text{O}$ and HNO_3 without H_3BO_3 (B7)

The hydrothermal reactions discussed in section 3.1.1 repeated without using H_3BO_3 in solution using the same conditions and procedure given on page 20. The white

powder obtained investigated by X-Ray and IR methods. Table 3.7 and Figure 3.10 shows the X-Ray data and pattern of the product dried at room temperature.

Table 3.7 XRD Data of the Product Obtained from $\text{AlCl}_3 \cdot 6\text{H}_2\text{O}$, $\text{Na}_4\text{P}_2\text{O}_7 \cdot 10\text{H}_2\text{O}$ and HNO_3 by Hydrothermal Reaction

I/I_0	d_{obs}
4	8.4928
100	4.2789
8	3.9942
32	3.3760
3	2.4752
3	2.3099
4	2.2561
74	2.1462
10	1.9956
4	1.8376
2	1.6856
2	1.6196
21	1.5528

Comparison the data in Table 3.7 showed that the d-spacings are about the same with the compound obtained with the mixture containing H_3BO_3 (B7 dried at room temperature). This proved that the inclusion of boron does not change the structure.

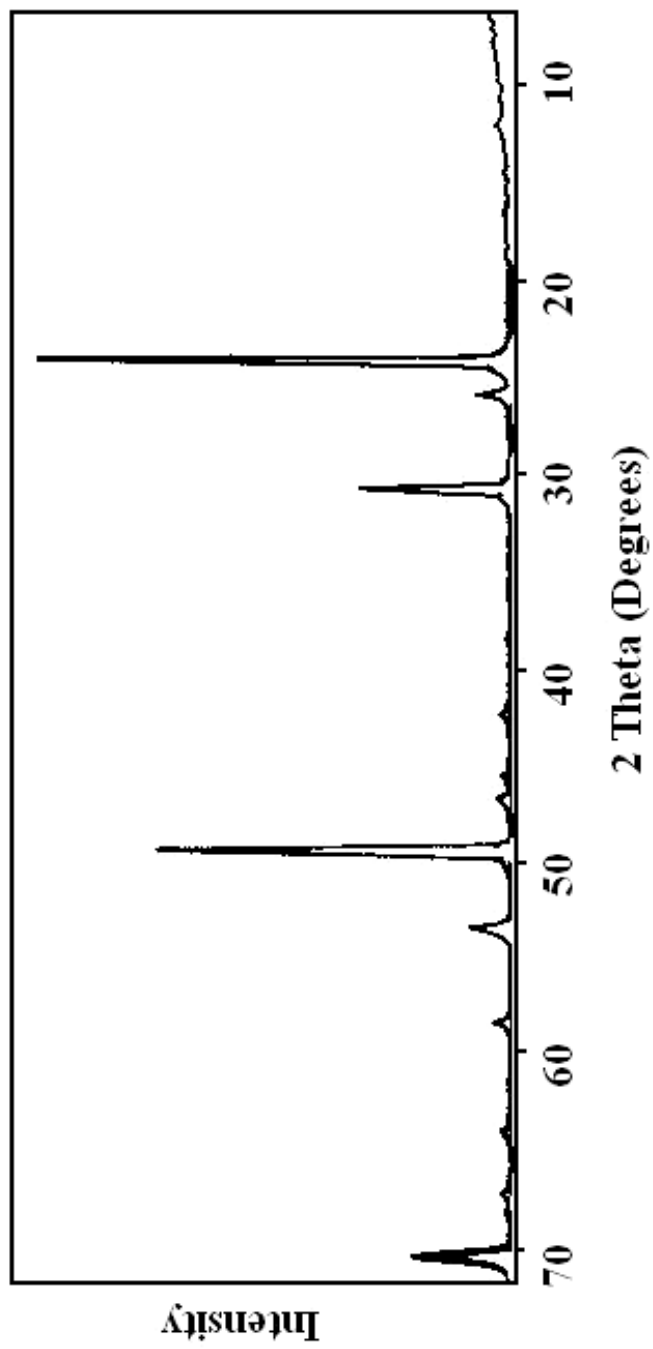


Figure 3.10 The IR Spectra of The product Obtained from $\text{AlCl}_3 \cdot 6\text{H}_2\text{O} + 5 \text{HNO}_3$
 $+ 2\text{Na}_4\text{P}_2\text{O}_7 \cdot 10\text{H}_2\text{O}$ Exp.No: B7

3.1.2 Hydrothermal Reaction of $\text{AlCl}_3 \cdot 6\text{H}_2\text{O}$, Na_2HPO_4 , H_3BO_3 and HCl (B3)

In this experiment, Al : B : P in a molar ratio 1 : 1 : 4 in acidic solution subjected to hydrothermal reaction at 180°C for a reaction period of 2 days. As a result of this hydrothermal reaction, a white powder was obtained. This product washed with distilled water and dried in air. In the powder diffraction pattern of the product, $\text{AlPO}_4 \cdot x\text{H}_2\text{O}$ (JCPDS Card No: 15-265), BPO_4 (JCPDS Card No: 34-132) and unknown weak lines were appeared (Figure 3.11). The X-Ray powder data of the product is given in Table 3.8.

The IR spectrum of the product (Figure 3.12), was found to be in good agreement with bands of PO_4 , BO_4 and BOP groups.

Table 3.8 The X-Ray Powder Diffraction Data of the Product Obtained from $\text{AlCl}_3 \cdot 6\text{H}_2\text{O}$, Na_2HPO_4 , H_3BO_3 and HCl Exp.No: B3

I/I_0	d_{obs}	$\sin^2\theta_{\text{obs}}$	Remark
11	7.3188	0.01496	$\text{AlPO}_4 \cdot x\text{H}_2\text{O}$
29	4.9234	0.03305	$\text{AlPO}_4 \cdot x\text{H}_2\text{O}$
8	4.5882	0.03806	$\text{AlPO}_4 \cdot x\text{H}_2\text{O}$
7	4.3589	0.04217	$\text{AlPO}_4 \cdot x\text{H}_2\text{O}$
6	4.3052	0.04323	–
100	3.9345	0.05176	$\text{AlPO}_4 \cdot x\text{H}_2\text{O}$
54	3.7000	0.05853	$\text{AlPO}_4 \cdot x\text{H}_2\text{O}$
13	3.6489	0.06018	BPO_4
11	3.4584	0.06699	$\text{AlPO}_4 \cdot x\text{H}_2\text{O}$
13	3.3976	0.06941	$\text{AlPO}_4 \cdot x\text{H}_2\text{O}$
7	3.1940	0.07854	$\text{AlPO}_4 \cdot x\text{H}_2\text{O}$
6	3.1240	0.08210	$\text{AlPO}_4 \cdot x\text{H}_2\text{O}$
10	2.9974	0.08918	$\text{AlPO}_4 \cdot x\text{H}_2\text{O}$

Table 3.8 Continued

25	2.8658	0.07955	AlPO ₄ .xH ₂ O
7	2.7955	0.10253	AlPO ₄ .xH ₂ O
20	2.7599	0.10519	AlPO ₄ .xH ₂ O
5	2.6489	0.11419	AlPO ₄ .xH ₂ O
23	2.5120	0.12697	AlPO ₄ .xH ₂ O
7	2.4532	0.13314	AlPO ₄ .xH ₂ O
4	2.3539	0.11460	–
7	2.2493	0.15836	BPO ₄
6	2.1751	0.16934	AlPO ₄ .xH ₂ O
5	2.1502	0.17329	–
5	2.1280	0.17694	–
4	2.0419	0.19217	–
4	1.9991	0.20049	–
7	1.9616	0.20831	–
4	1.9192	0.21752	–
9	1.8654	0.23025	BPO ₄
5	1.8478	0.23467	–
4	1.7997	0.24736	–
3	1.7821	0.252271	–
5	1.7342	0.26642	–
5	1.6479	0.29504	–
8	1.5864	0.31837	–
8	1.5471	0.33474	–
6	1.5247	0.34466	–

The weak lines belong to an unknown compound. This could be due to trace amount of (%5-10) Al_{3-x}B_xP₄O₁₃.

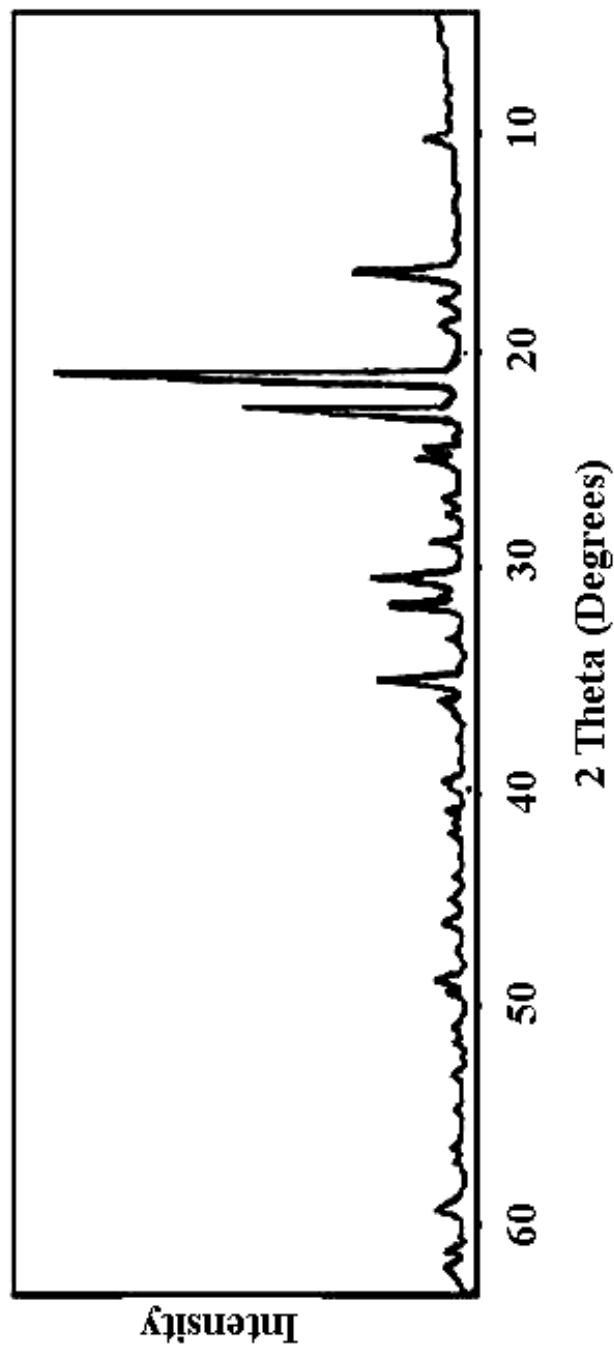


Figure 3.11 The XRD pattern of the Product Obtained from $\text{AlCl}_3 \cdot 6\text{H}_2\text{O}$, Na_2HPO_4 , H_3BO_3 and HCl Exp.No: B3

The IR spectrum of the product (Figure 3.12), was found to be in good agreement with bands of PO₄, BO₄ and BOP groups. The assignments of IR data is given in Table 3.9.

Table 3.9 Assignments for the IR Spectra of the Product for Exp. No: B3

Frequency (cm ⁻¹)	Assignment
3347	ν (OH) stretching in H ₂ O
3162	Hydrogen bonding
1600	OH deformation in H ₂ O
1238	ν _{as} PO ₂ (OPO)
1192, 1142	ν _s PO ₂ (OPO)
1115	ν ₃ PO ₄ , ν ₃ BO ₄
782	ν _s P-O-P in polyphosphates or B-O-P in borophosphates, pseudo lattice Al-O vibrations
753	ν _s P-O-P in polyphosphates or B-O-P in borophosphates, pseudo lattice Al-O vibrations
716	ν _s P-O-P in polyphosphates or B-O-P in borophosphates, pseudo lattice Al-O vibrations
664, 500	ν ₄ PO ₄ , δ PO ₂ , ν ₄ BO ₄
451, 413	ν ₂ in PO ₄ , δ PO ₂

The IR data agreed quite well with BPO₄, AlPO₄ and the frequencies given for P₄O₁₃⁶⁻ ion by Uztetik et al [83]. On the other hand AlPO₄ is composed of (PO₄)³⁻ and (AlO₄)⁵⁻ tetrahedras, but in this framework P-O and Al-O bondings are different depending on electronegativities [87-88]. Al-O bonds are predominantly ionic and P-O bonds covalent. In this case we expect lattice vibrations as well as tetrahedrally coordinated Al³⁺ ion vibrations (pseudo lattice vibrations) at about 708cm⁻¹ [87]. Lattice vibrations happened to be below 400 cm⁻¹ which we could not observe due to instrumental limitations.

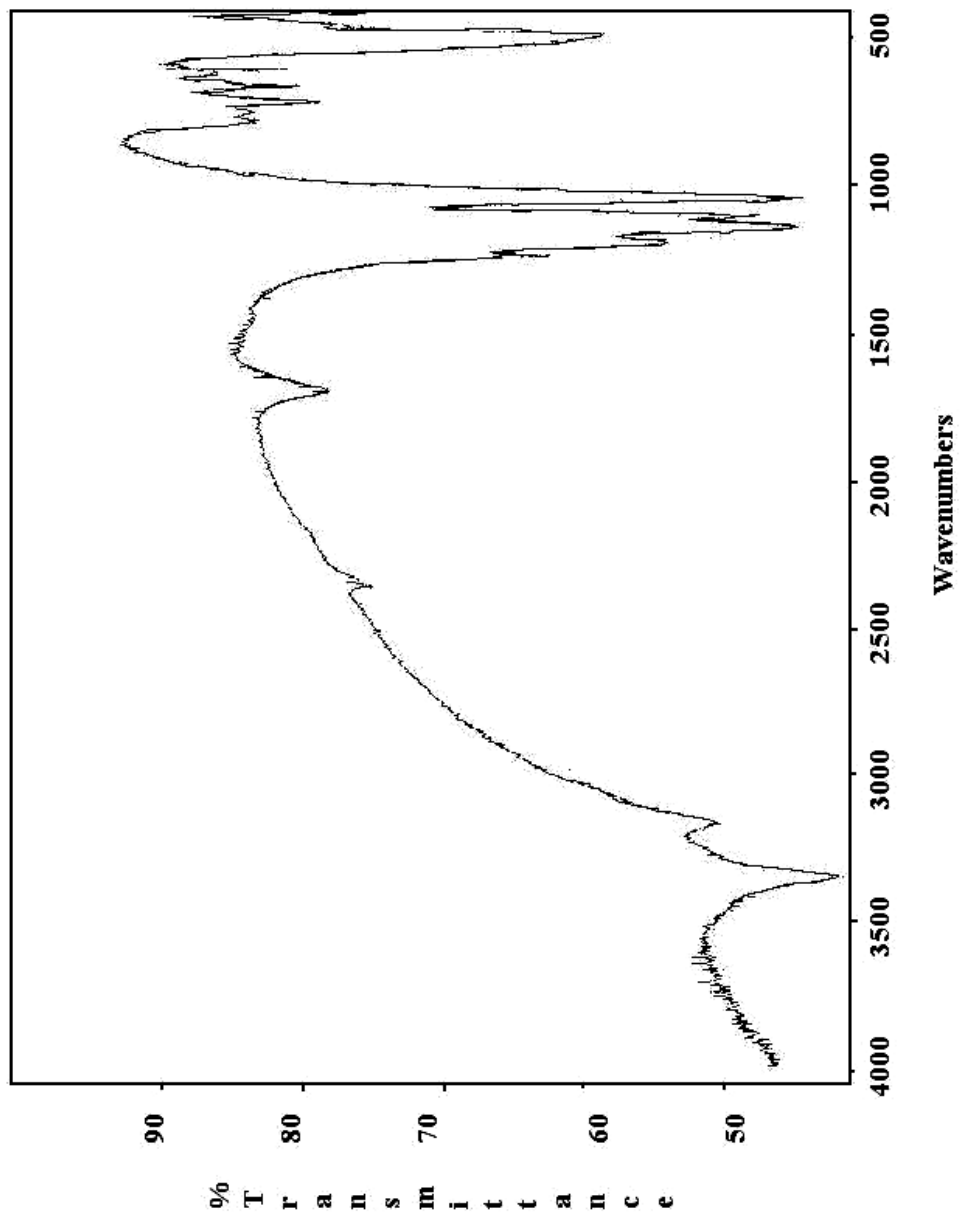


Figure 3.12 The IR Spectra of the Product Obtained from $\text{AlCl}_3 \cdot 6\text{H}_2\text{O}$, Na_2HPO_4 , H_3BO_3 and HCl Exp.No: B3

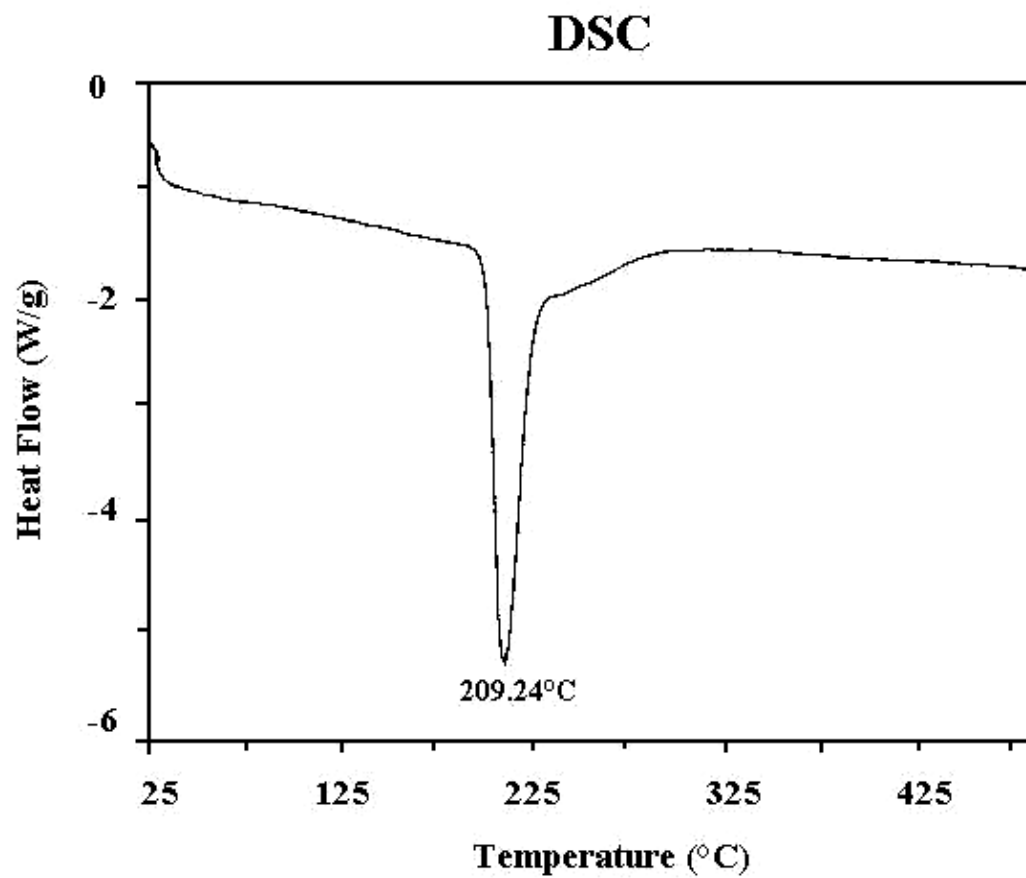


Figure 3.13 DSC study of the Product Obtained from $\text{AlCl}_3 \cdot 6\text{H}_2\text{O}$, Na_2HPO_4 , H_3BO_3 and HCl Exp.No: B3

DSC pattern Figure 3.13 corresponds the loss of crystal water at 209.24°C.

3.2 Solid State Reactions

3.2.1 Solid State Reaction of Al₂O₃, B₂O₃ and (NH₄)₂HPO₄

The reaction was performed at 800-1140°C for different periods of time. Experimental conditions for this reaction is summerized in Table 3.10.

Table 3.10 Experimental Conditions of the Product Obtained from Al₂O₃, B₂O₃ and (NH₄)₂HPO₄ Exp.No: A1

T (°C)	Time (hour)	Remark
800	8	BPO ₄ + Al(PO ₃) ₃
900	22	BPO ₄ + Al(PO ₃) ₃
990	15	BPO ₄ + Al(PO ₃) ₃
1140	10	melt(glass)

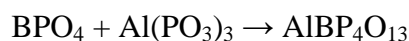
In the XRD patterns of the products at 800-990°C BPO₄ (JCPDS Card No.34-132) and Al(PO₃)₃ (JCPDS Card No.13-264) lines were found. At 1140°C the product melted so it was impossible to complete the reaction at high temperatures.

The weight loss is in agreement with the theoretical value (% 63.82 observed, %62.89 theoretical).

The probable reaction is



If we would go to higher temperatures



reaction should happen, but at 1140°C it becomes glass with the probable formula of AlBP₄O₁₃. This observation proved the statement ‘ tetrapolyphosphates are rare and difficult to crystallize’ since Bennezha et al [86] prepared Ba₃P₄O₁₃ by fusion methods.

Table 3.11 XRD Data of the Product Obtained by the Solid State Reactions at Different Temperatures (Exp.No. A1)

800 °C		900 °C		990 °C	
I/I ₀	d _{obs}	I/I ₀	d _{obs}	I/I ₀	d _{obs}
7	5.3127 *	–	–	8	5.3261 *
7	5.1547 *	–	–	–	–
–	–	11	4.3499	16	4.3409
11	3.9641	91	3.9272	–	–
–	–	–	–	100	3.8766
46	3.7998	–	–	–	–
100	3.6301 •	100	3.6364 •	77	3.6364 •
–	–	10	3.4250	10	3.4360
36	3.3442 *	–	–	9	3.3495 *
–	–	9	3.3233	–	–
7	3.1988 *	–	–	–	–
7	3.1149 *	–	–	–	–
7	3.0703 •	12	3.0703 •	9	3.0703 •
14	3.0142 *	–	–	–	–
–	–	–	–	6	2.9933
–	–	7	2.9281	7	2.9202
6	2.8735	–	–	–	–
6	2.7991	–	–	–	–
7	2.7321	–	–	–	–
7	2.6716	7	2.6915	6	2.6881
–	–	10	2.4024	–	–
9	2.3792	–	–	12	2.3792
34	2.2538 •	33	2.2561 •	27	2.2538 •
6	2.1794	–	–	–	–

Table 3.11 Continued

–	–	6	1.9683	5	1.9683
11	1.8669 [•]	12	1.8654 [•]	11	1.8654 [•]
7	1.8178 [•]	7	1.8178 [•]	6	1.8178 [•]

(* : Al(PO₃)₃, • : BPO₄)

The IR data of the products at 800 °C and 990 °C are given in Table 3.12.

Table 3.12 IR Frequencies of The Product (A1) at 800 °C and 990 °C

800 °C		990 °C
Frequency (cm ⁻¹)	Assignments	Frequency (cm ⁻¹)
1276, 1250	ν_{as} PO ₂ in PO ₃	–
1100	BPO ₄ , ν_s PO ₂ in PO ₃	1090, 1037
932	BPO ₄	–
772, 727	P-O-P in metaphosphates	740
625, 607	BPO ₄ , δ PO ₂ in PO ₃	607
552	BPO ₄	540
439	δ PO ₂ in PO ₃	454

The IR data shows some distortions and broadening in BPO₄ spectrum. This may be due to the new compound being a glass ceramic containing BPO₄ lines.

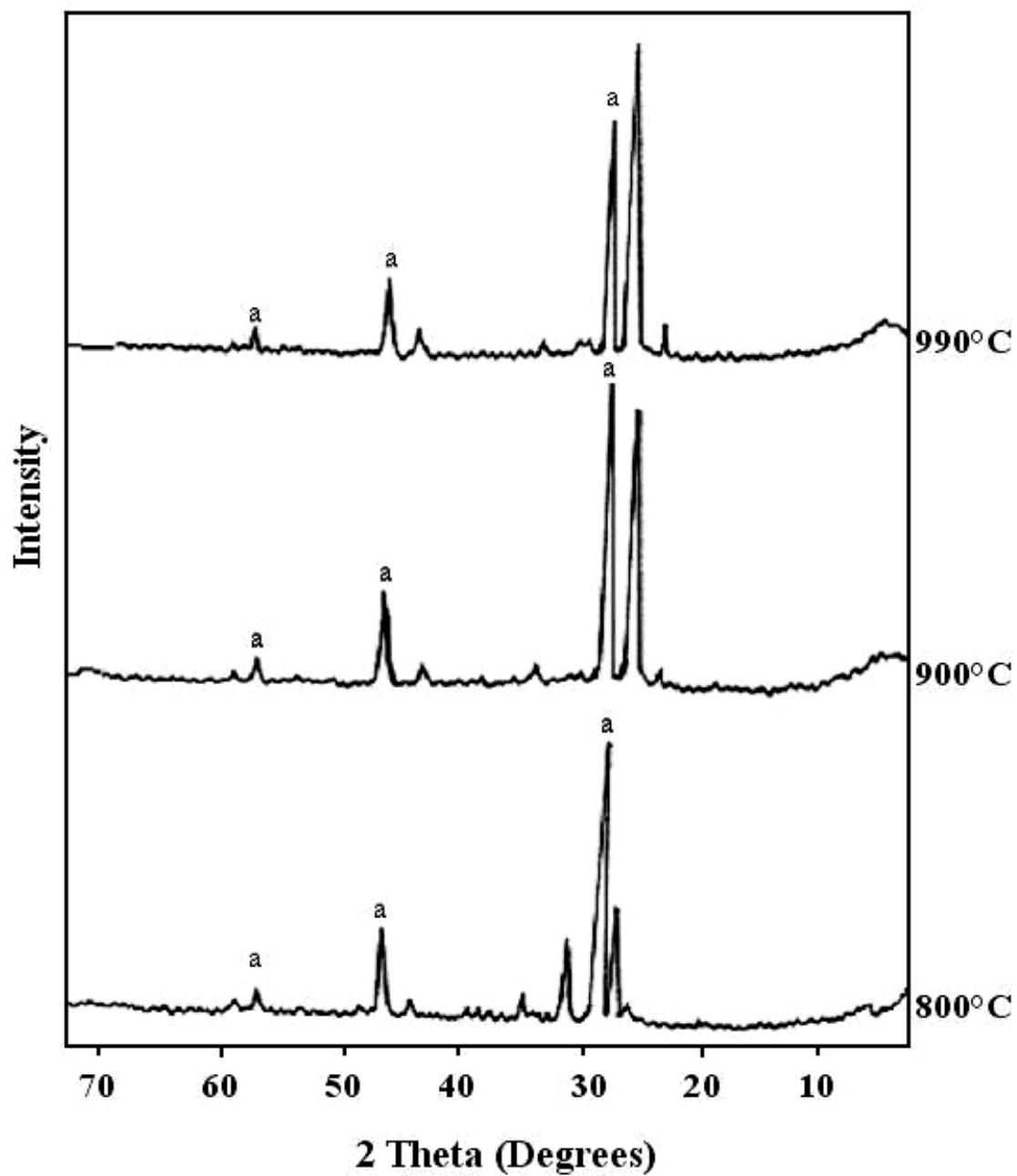


Figure 3.14 The XRD pattern of The Product Obtained from Al_2O_3 , B_2O_3 and $(\text{NH}_4)_2\text{HPO}_4$ Exp.No: A1 (where a = BPO_4)

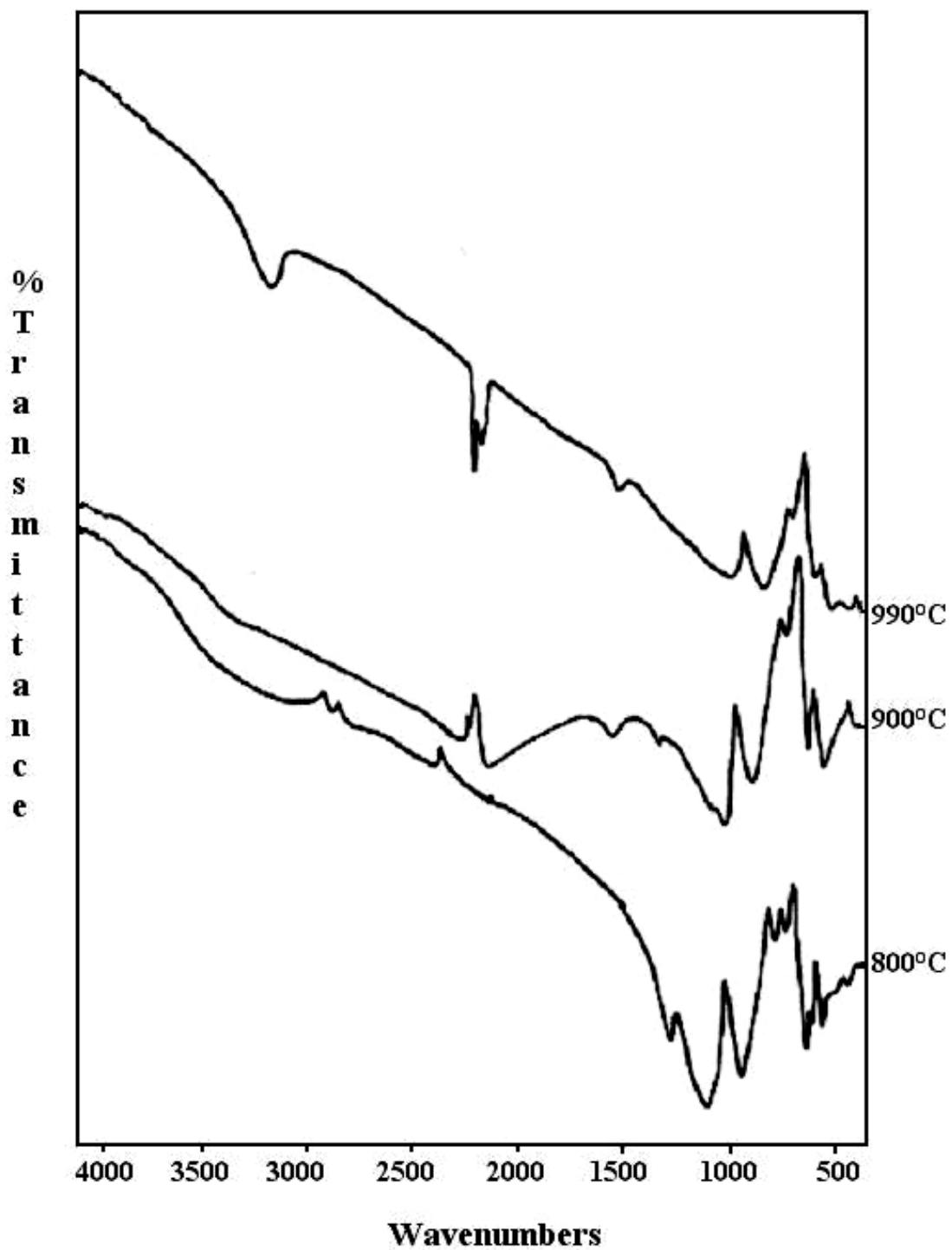


Fig.3.15 The IR Spectra of The Product Obtained from Al_2O_3 , B_2O_3 and $(\text{NH}_4)_2\text{HPO}_4$

Exp.No: A1

3.2.2 Synthesis of Boron and Phosphorus Containing Anorthite (A4)

In the synthesis of boron and phosphorus containing anorthite as discussed in experimental section (page 21) two different solid state reactions were performed.

a) In the first reaction CaCO_3 , Al_2O_3 , B_2O_3 and $(\text{NH}_4)_2\text{HPO}_4$ were subjected to solid state reaction at 700, 800, 900, 1000 and 1200 °C for a period of 8, 12, 11, 14 and 5 hours to synthesize $\text{CaAl}_2\text{BPO}_8$ (A4).

The predicted reaction is:



In anorthite Al has an octahedral and Si has tetrahedral coordination. We expect the same structure since Si positions are replaced by B and P. For the solid state reaction at 700 °C (A4 700) and reaction was not completed. A very complex pattern was obtained by XRD which contain condense phosphates (metaphosphates), orthophosphates of calcium, boron phosphate and borates (Figure 3.16). The IR data was pretty clear having frequencies due to PO_3^{1-} , PO_4^{3-} , $\text{P}_n\text{O}_{3n+1}^{(n+2)-}$ (polyphosphate), BO_3^{3-} , BO_4^{5-} , Al-O and CO_3^{2-} but it was difficult to do assignments. Figure 3.17 shows the IR spectra.

Solid State Reaction at 800 °C (A4 800)

In the XRD data stronger lines were observed with respect to product obtained at 700 °C. BPO_4 was not present. The four strong lines are 2.87, 4.11, 3.35 and 2.58 Å. Examination of the d-spacings revealed that the pattern contain several products which was difficult to identify (Figure 3.16). The IR data (Figure 3.17) shows weak metaphosphate, but strong condense phosphate modes.

Solid State Reaction at 900°C (A4 900)

The XRD pattern of the product obtained at this temperature was different from the product obtained at 800°C. Strong lines appeared at 4.08, 2.86 and 2.58 Å. The data can not be indexed. The IR data is much more simple showing BO₄, PO₄ and B-O-P modes (Figure 3.17).

Solid State Reaction at 1000°C (A4 1000)

In this case weight loss was in agreement with the theoretical value (%28.72 observed, %26.98 theoretical). The XRD data at 400 cps was given Table 3.13. The strong lines (4.0953, 2.8658, 2.5800) were in agreement with the values obtained in 900°C pattern).

Table 3.13 The X-Ray Powder Diffraction Data of the Product Obtained from CaCO₃, Al₂O₃, B₂O₃ and (NH₄)₂HPO₄ (Exp.No: A4 1000°C)

I/I₀	d_{obs}
31	8.0931
33	6.4921
41	5.1803
100	4.0953
31	3.4528
57	3.1750
14	2.9767
92	2.8658
20	2.7321
16	2.6716
57	2.5800

Table 3.13 Continued

31	2.5034
14	2.3869
16	2.1710
23	2.1482
25	1.9161
18	1.8774
14	1.8610
37	1.7217
18	1.5358

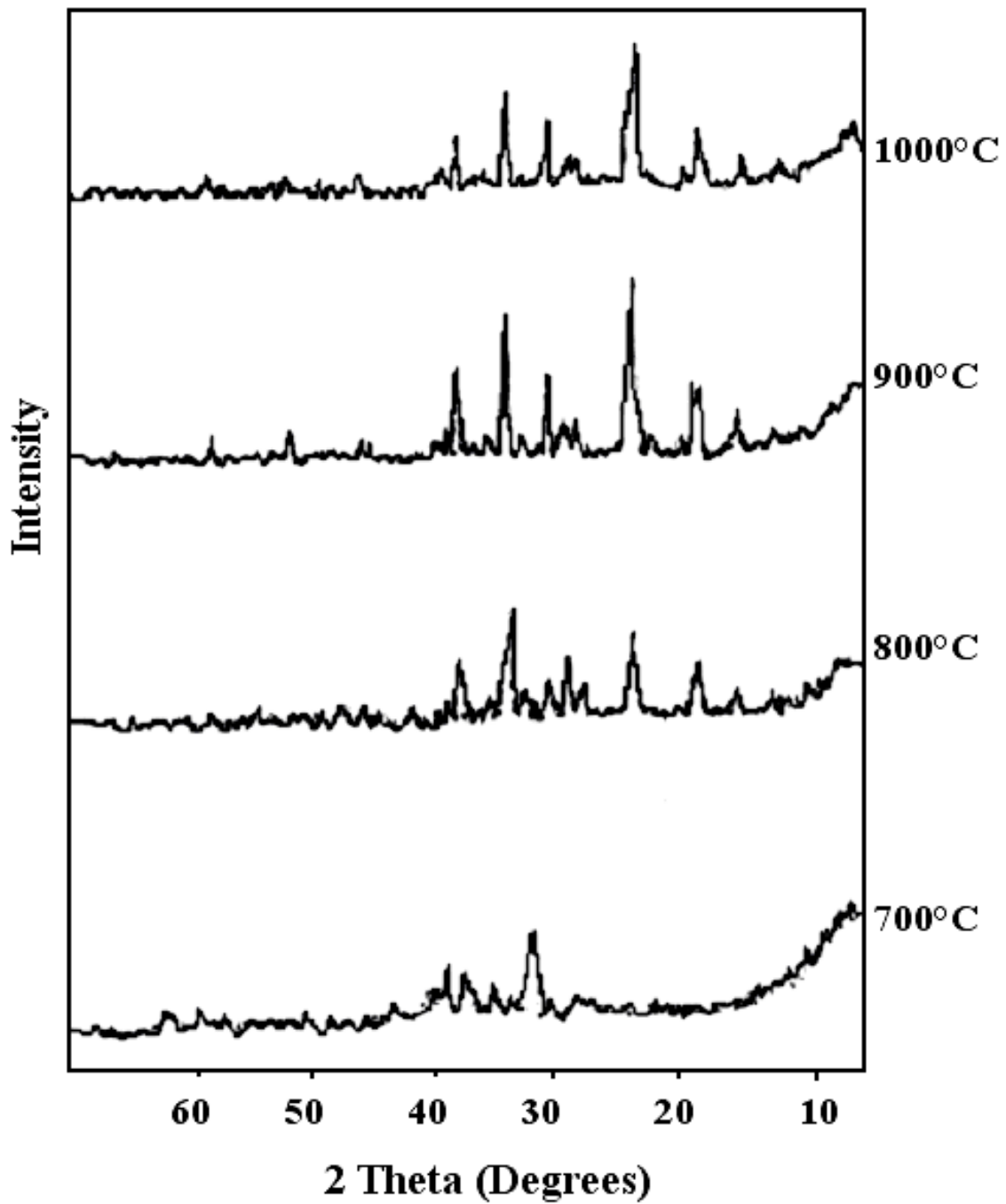


Figure 3.16 The XRD pattern of the Product Obtained from CaCO_3 , Al_2O_3 , B_2O_3 and $(\text{NH}_4)_2\text{HPO}_4$ Exp.No: A4

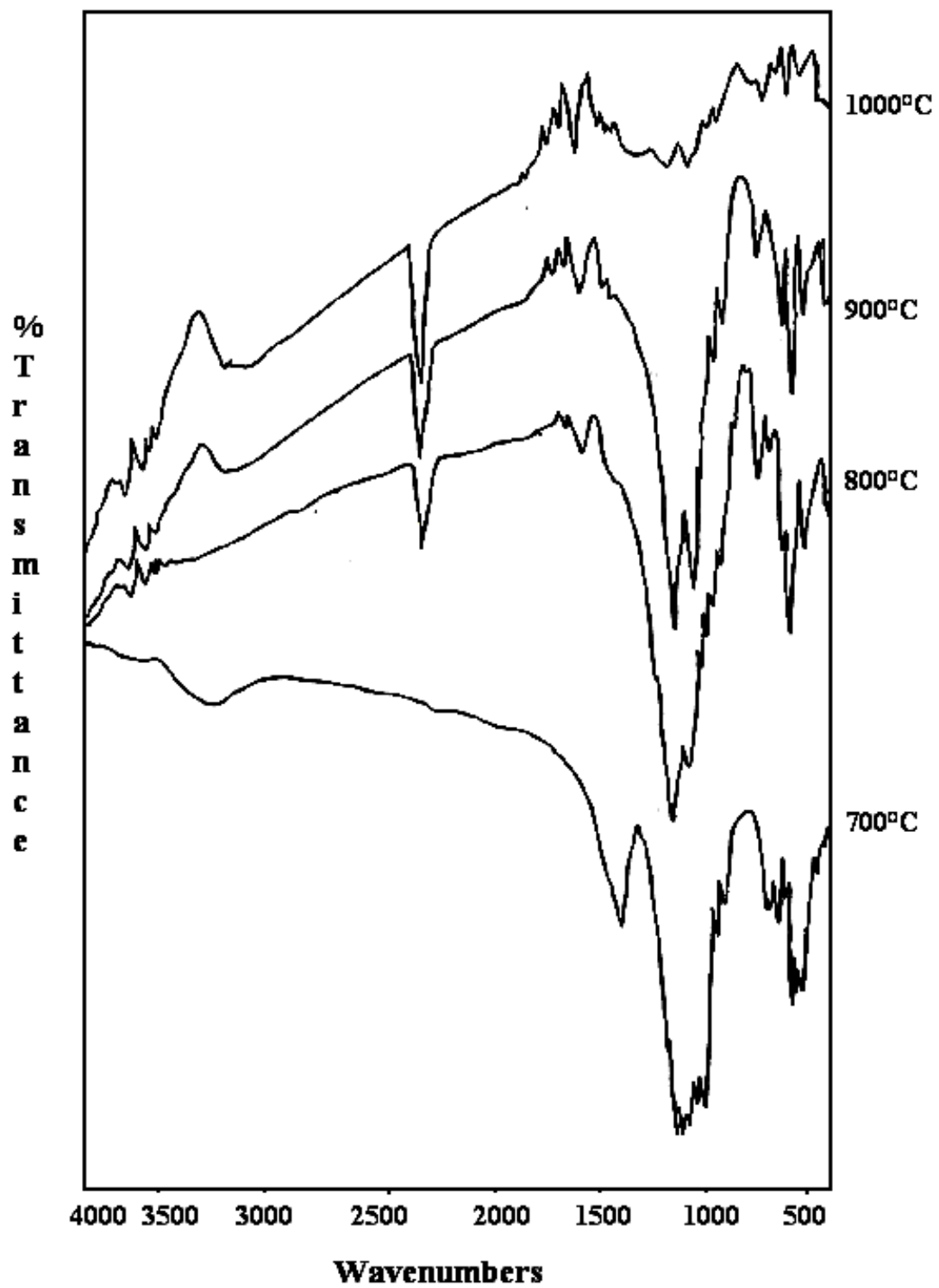


Figure 3.17 The IR Spectra of the Product Obtained from CaCO_3 , Al_2O_3 , B_2O_3 and $(\text{NH}_4)_2\text{HPO}_4$ Exp.No: A4

b) In the second method instead of CaCO₃, CaO was used in the solid state reaction given by the following equation:



Depending on the previous results this reaction was performed at 1000°C (A5 1000). The XRD pattern was taken at 400 and 100 cps to see the weak reflections. The pattern was in agreement with the A4 1000 pattern. The XRD pattern of A5 1000 was indexed in the monoclinic system and reported in Table 3.14. The A, B, C and D values are found to be as:

A = 0.00795, B = 0.00500, C = 0.00385 and D = 0.00060 using these values computer calculations gave the following unit cell parameters a = 10.04402 Å, b=12.65873 Å, c = 14.43323 Å and β = 91.55°.

Table 3.14 X-Ray Diffraction Data of Boron and Phosphorus Containing Anorthite, CaAl₂BPO₈ (sample A5 1000°C)

Monoclinic a = 10.04402, b = 12.65873, c = 14.43323 and β = 91.55°.

I/I ₀	2θ	d _{obs}	sin ² θ _{obs}	sin ² θ _{cal}	hkl
7	7.10	14.4560	0.00384	0.00385	001
5	8.20	12.5210	0.00511	0.00500	010
11	10.25	10.0203	0.00798	0.00795	100
10	10.80	9.5117	0.00882	0.00885	011
13	12.70	8.0931	0.01223	0.01240	101
9	13.14	7.8234	0.01309	0.01298	110
6	14.20	7.2419	0.01528	0.01540	002
5	14.74	6.9781	0.01648	0.01680	11-1
5	15.25	6.7599	0.01761	0.01740	111
19	16.00	6.4318	0.01937	0.02000	020

Table 3.14 Continued

16	16.40	6.2759	0.02034	0.02040	012
5	16.90	6.0916	0.02159	0.02125	102
5	17.75	5.8150	0.02380	0.02365 0.02385	10-2 021
19	19.15	5.3812	0.02767	0.02795 0.02715	120 11-2
20	19.95	5.1675	0.03000	0.02955	112
6	20.90	4.9352	0.03290	0.03321	20-1
3	21.45	4.8100	0.03463	0.03465	003
6	21.75	4.7445	0.03560	0.03540	022
8	23.30	4.4326	0.04080	0.04078	103
34	23.70	4.3589	0.04217	0.04215	122
6	24.35	4.2444	0.04448	0.04440	10-3
6	24.40	4.2358	0.04466	0.04455 0.04500	12-2 030
6	24.45	4.2273	0.04485	0.04480	20-2
100	25.35	4.0795	0.04815	0.04855	031
18	26.70	3.8767	0.05331	0.05295	130
6	27.50	3.8205	0.05649	0.05670	131
7	28.65	3.6178	0.06122	0.06180	004
7	29.30	3.5393	0.06397	0.06440	123
15	30.10	3.4473	0.06742	0.06800	13-2
8	30.60	3.3923	0.06965	0.06965	222
9	30.90	2.3600	0.07097	0.07095	11-6
9	30.95	3.3548	0.07119	0.07140	20-3
9	31.60	3.2874	0.07414	0.07360	30-1
7	32.20	3.2279	0.07690	0.07720	301
34	32.75	3.1750	0.07948	0.07965	033

Table 3.14 Continued

32	32.80	3.1704	0.07972	0.08000	040
10	34.90	2.9850	0.08992	0.08980	23-2
10	35.10	2.9686	0.09093	0.09120	14-1
5	35.75	2.9045	0.09421	0.09460	232
60	36.40	2.8659	0.09755	0.09715	321
12	38.25	2.7321	0.10734	0.10665	31-3
7	39.1	2.6749	0.11198	0.11180	240
40	40.55	2.5830	0.12008	0.11960	33-1
20	41.80	2.5091	0.12726	0.12720	400
5	44.15	2.3818	0.14124	0.14160	044
3	45.40	2.3196	0.14890	0.14865	42-1
6	46.75	2.2562	0.15741	0.15780	42-2
				0.16980	43-1
15	48.70	2.1710	0.17000	0.17055	342
12	49.25	2.1480	0.17362	0.17460	431
3	50.30	2.1062	0.18062	0.18080	34-3
4	51.50	2.0585	0.18874	–	–
9	52.75	2.0149	0.19736	–	–
7	55.85	1.9113	0.21932	–	–
7	57.05	1.8744	0.22805	–	–
8	52.70	1.8551	0.23282	–	–
4	59.00		0.24256	–	–
7	59.80	1.7956	0.24849	–	–
15	62.80	1.7180	0.27145	–	–

The last 8 lines were not indexed, since this region is pretty sensitive to measurements and it is very difficult to index powder XRD pattern for monoclinic system in the high angle region.

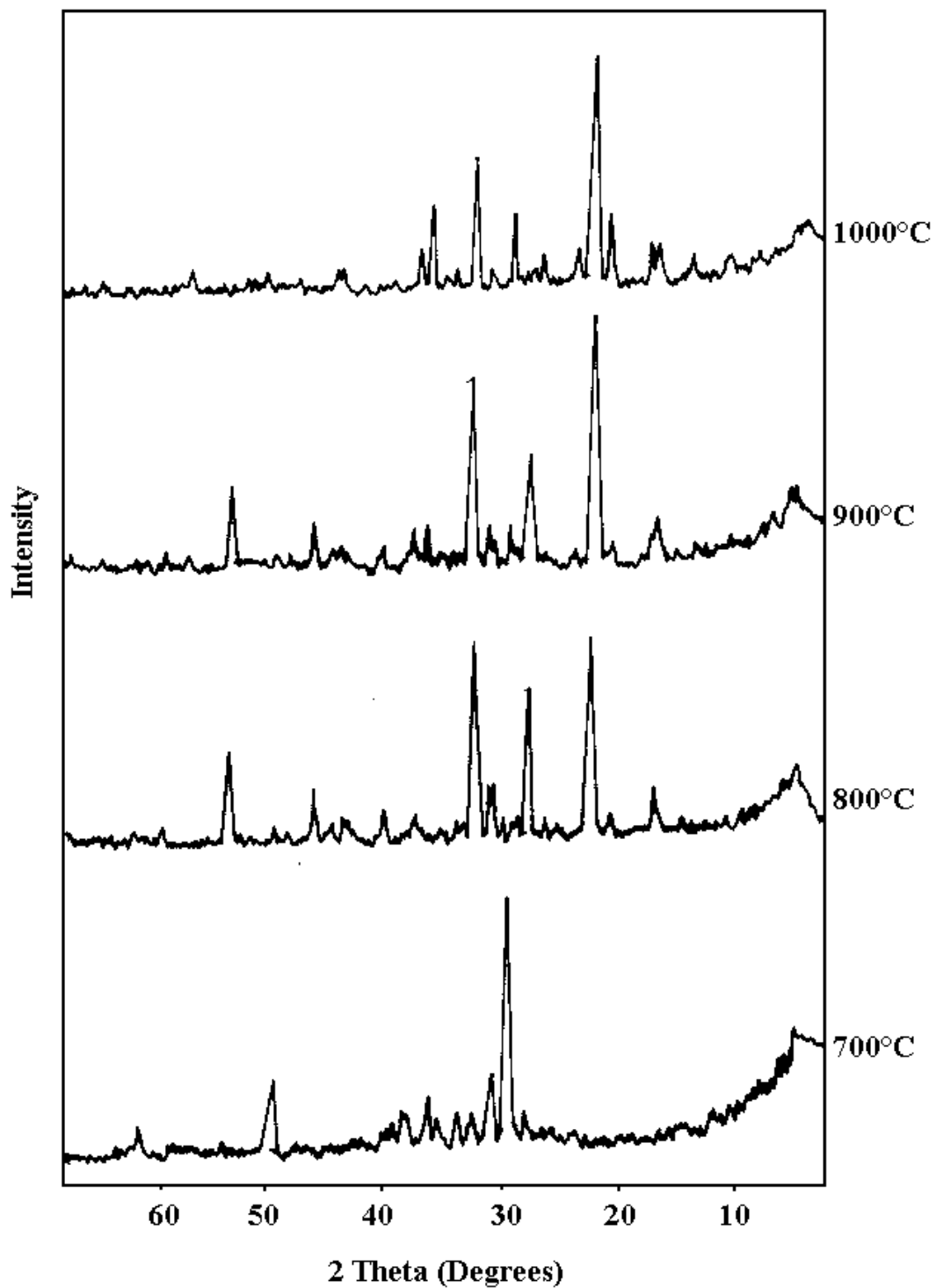


Figure 3.18 The XRD pattern of the Product Obtained from CaO, Al₂O₃, B₂O₃ and (NH₄)₂HPO₄, Exp.No: A5

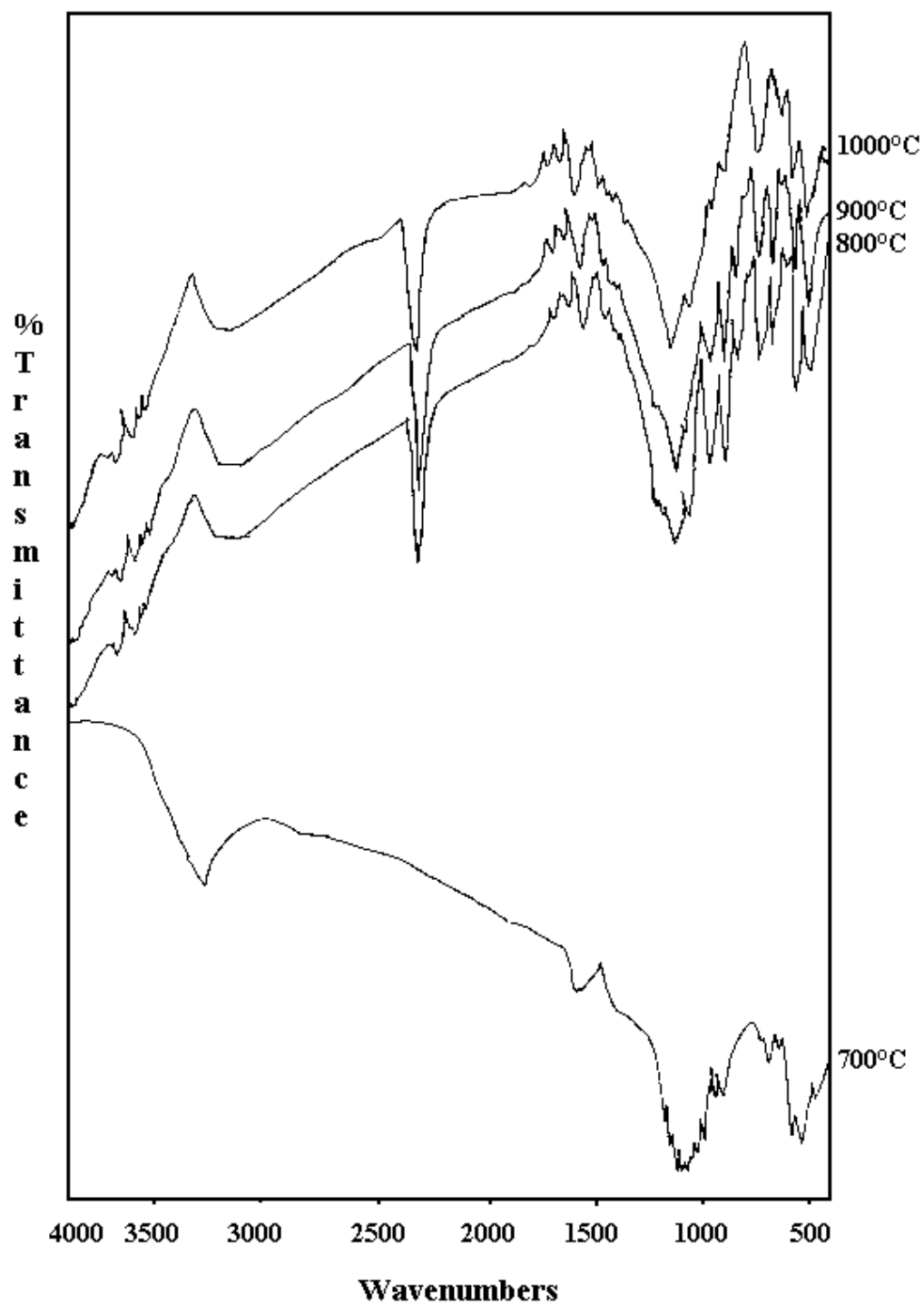


Figure 3.19 The IR Spectra of the Product Obtained from CaO, Al₂O₃, B₂O₃ and (NH₄)₂HPO₄, Exp.No: A5

Experimental conditions and the results obtained from two methods is summerized in Table 3.15.

Table 3.15 Experimental Conditions for the Synthesis of Boron and Phosphorus Containing Anorthite

CaCO₃, B₂O₃, Al₂O₃, (NH₄)₂HPO₄ (A4) CaO, B₂O₃, Al₂O₃, (NH₄)₂HPO₄ (A5)

T (°C)	Time (hour)	Remark	T (°C)	Time (hour)	Remark
700	8	unidentified	700	8	unidentified
800	12	unidentified	800	12	unidentified
900	11	unidentified	900	11	unidentified
1000	14	boron and phosphorus containing anorthite	1000	14	boron and phosphorus containing anorthite
1200	5	melt (glass)	1200	5	melt (glass)

The IR frequencies of the product obtained through the solid state reactions of CaO, Al₂O₃, B₂O₃ and (NH₄)₂HPO₄ (A5 1000°C) are given in Table 3.16.

Table 3.16 IR Frequencies of The Product Obtained from CaO, Al₂O₃, B₂O₃ and (NH₄)₂HPO₄, Exp.No: A5 (1000°C)

Frequencies (cm ⁻¹)	Assignment
1260	ν P=O
1132	ν_3 BO ₄ , ν_3 PO ₄
1038	ν_3 PO ₄
950	ν_1 PO ₄
884	ν_{as} B-O-P

Table 3.16 Continued

731, 710	ν_s B-O-P, Al-O
660	δ B-O-P, Al-O
629	Al-O-Al, Al-O
601	δ B-O-P
556	δ O-P-O
494	ν_2 PO ₄
476, 425	ν_2 PO ₄

Examining all the data proved that the product is CaAl₂BPO₈.

CHAPTER IV

CONCLUSION

The object of this research was to synthesize some novel aluminum and calcium borophosphate compounds and characterize them. For this purpose

a) Several compositions of Al_2O_3 , $(\text{NH}_4)_2\text{HPO}_4$ and H_3BO_3 were subjected to hydrothermal and solid state reactions at different temperatures.

b) Solid state reactions of CaCO_3 or CaO with Al_2O_3 , B_2O_3 and $(\text{NH}_4)_2\text{HPO}_4$ compositions were investigated at different temperatures to obtain boron and phosphorus containing anorthite.

In the hydrothermal reactions the predicted compound $\text{AlBP}_4\text{O}_{13}$ was not obtained. After examining the air dried and products heated at different temperatures revealed the formation of $\text{Al}_{3-x}\text{B}_x\text{P}_3\text{O}_{12}$. The formula was proved by XRD, IR, DTA, EDX and SEM methods. The unit cell dimensions were calculated as $a = 17.1629\text{Å}$ and $c = 12.6084\text{Å}$ with the space group $\text{P}4_21_2$ (No.90).

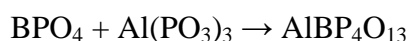
Hydrothermal reactions repeated without H_3BO_3 and it was seen that the d-spacings are about the same with the compound obtained with the mixture containing H_3BO_3 , so it was decided that the inclusion of boron does not change the structure.

The hydrothermal reactions of $\text{AlCl}_3 \cdot 6\text{H}_2\text{O}$, Na_2HPO_4 , H_3BO_3 with HCl produced $\text{AlPO}_4 \cdot x\text{H}_2\text{O}$ while trying to synthesize $\text{AlBP}_4\text{O}_{13}$. The powder diffraction pattern of the product was in agreement with the $\text{AlPO}_4 \cdot x\text{H}_2\text{O}$ (JCPDS Card No: 15-265). In the powder diffraction pattern, also BPO_4 (JCPDS Card No: 34-132) and unknown weak lines were appeared. The weak lines could be due to trace amount of (%5-10) $\text{Al}_{2-x}\text{B}_x\text{P}_4\text{O}_{13}$. The IR spectrum of the product was found to be in good agreement with bands of PO_4 , BO_4 and BOP groups.

$\text{Al}(\text{PO}_3)_3$ was obtained by the solid state reaction of Al_2O_3 , B_2O_3 and $(\text{NH}_4)_2\text{HPO}_4$. The probable reaction is



At 1140°C the product was melted. If we could go to higher temperatures



reaction should happen, with the probable formula of $\text{AlBP}_4\text{O}_{13}$.

Boron and phosphorus containing anorthite was synthesized by the solid state reactions. Two different reactions were performed. In the first reaction CaCO_3 , Al_2O_3 , B_2O_3 and $(\text{NH}_4)_2\text{HPO}_4$ were used and in the second method instead of CaCO_3 , CaO was used. The products of these reactions gave the same XRD pattern and it was indexed in the monoclinic system with the following unit cell parameters $a = 10.04402\text{Å}$, $b = 12.65873\text{Å}$, $c = 14.43323\text{Å}$ and $\beta = 91.55^\circ$. Examining all the data proved that the product is $\text{CaAl}_2\text{BPO}_8$.

REFERENCES

- [1] M. T. Averbuch-Pouchot and A. Durif, Topics in Phosphate Chemistry, 1996.
- [2] P. J. Flory, Statistical Mechanics of Chain Molecules, Wiley-Interscience, New York, 1969.
- [3] D. E. C. Corbridge, Phosphorous: An Outline of its Chemistry, Biochemistry, and Technology, Elsevier, Amsterdam, 4th edn., 1990.
- [4] D.E.C. Corbridge, Phosphorus: An Outline of its Chemistry, Analyst 121, 1089-1093, 1996. Biochemistry and Technology, Elsevier, Amsterdam, 5th ed. 172, 217-222, 1995.
- [5] K. H. Lii, Y. B. Chen, C. C. Su and S. L. Wang, J. Solid State Chem., 82, 156-160, 1989.
- [6] A. V. Lavrov, V. P. Nikolaev, G. G. Sadikov and M. Ya. Voitenko, Dokl. Akad. Nauk SSSR, 259, 103-106, 1981.
- [7] N. N. Chudinova, K. K. Palkina, N. B. Komarovskaya, S. I. Maksimova and N. T. Chibiskova, Dokl. Akad. Nauk SSSR, 306, 635-638, 1989.
- [8] A. Hamadi and T. Jouini, J. Solid State Chem., 111, 443-446, 1994.
- [9] J. Cotter-Howells, Environ Pollut., 93, 9 – 16, 1996.
- [10] G. M. Hettiarachchi, G. M. Pierzynski, M. D. Ransom, Environ Sci Technol., 34, 4614 – 4619, 2000.
- [11] Q. Y. Ma, S. J. Traina, T. J. Logan TJ, J. A. Ryan, Environ Sci Technol., 28, 1219 – 1228, 1994.
- [12] J. A. Ryan, P. Zhang, D. Hesterberg, J. Chou, D. E. Sayers, Environ Sci Technol., 35, 3798 – 3803, 2001.
- [13] Q. Y. Ma, S. J. Traina, T. J. Logan, Environ Sci Tech., 27, 1803 – 1810, 1993.

- [14] L. Q. Ma, G. N. Rao, *J. Environ Qual.*, 26, 788 – 794, 1997.
- [15] V. Laperche, T. J. Logan, P. Gaddam, S. Traina, *Environ Sci Technol.*, 31, 2745 – 2753, 1997.
- [16] V. P. Evangelou, *Int J Surf Min Reclamation Environ.*, 10, 135 – 142, 1996.
- [17] W. Ruigang, P. Wei, C. Jian, F. Minghao, C. Zhenzhu and L. Yongming, *Materials Chemistry and Physics*, 79, 30–36, 2003.
- [18] M. Kızılyallı and A. J. E. Welch, *The Chemistry and Structure of Rare Earth Phosphates*, PhD Thesis, London University, 1973.
- [19] M. Kızılyallı and A. J. E. Welch, *Rare Earths in Modern Science and Technology*, New York, 1, 209, 1978.
- [20] M. Kızılyallı and A. J. E. Welch, *J. Bid.*, 2, 59, 1980.
- [21] M. Kızılyallı, A. Sungur and D. C. Jones, *J. Lum. Common Metals*, 110, 249, 1985.
- [22] B. Finke, L. Schwarz, P. Gurtler, M. Kraas, M. Joppien, S. Becker, *J. Lumin.* 60/61, 975, 1994.
- [23] L. Schwarz, B. Finke, M. Kloss, A. Rohmann, U. Sasum, D. Haberland, *J. Lumin.*, 257, 72–74, 1997.
- [24] P. P. Melnikov, V. B. Kalinin, V. A. Efremov, L. N. Kommisarowa, *Iz. Akad. Nauk SSR, Neorg. Mater.*, 17, 1452, 1981.
- [25] C. E. Bamberger, P. R. Robinson, R. L. Sherman, *Inorg. Chim. Acta*, 34, L203, 1979.
- [26] H. Y.-O. Hong, S. R. Chinn, *Mater. Res. Bull.*, 11, 421, 1976, and references cited therein.
- [27] J. Zahletho, P. Houenou, R. Eholie, *Solid State Chem.*, C.R. Acad. Sci. Paris 397 (Ser. II) 1177, 1998.
- [28] M. Kloss, L. Schwarz, J.P.K. Holsa, *Acta Phys.*, 95, 343, 1999.
- [29] Z. J. Chao, C. Parent, G. Le Flem, P. Hagenmuller, *J. Solid State Chem.*, 82, 255, 1989.
- [30] R. Salmon, C. Parent, M. Vlasse, G. Le Flem, *Mater. Res. Bull.*, 13, 439, 1978.
- [31] Y. Sargin, M. Kızılyallı, C. Telli and H. Güler, *J. Eur. Ceram. Soc.*, 17 (7), 963-970, 1997.

- [32] L.L. Hench, J. Wilson, *An Introduction to Bioceramics*, World Scientific, New Jersey/London/Singapore, 1993.
- [33] R.Z. LeGeros, in: H. Myers (Ed.), *Calcium Phosphates in Oral Biology and Medicine. Monographs in Oral Science*, vol. 15, S. Karger AG, Basel, 1991.
- [34] H. Aoki, *Science and Medical Applications of Hydroxyapatite*, Japanese Association of Apatite Science, Tokyo, 1991.
- [35] J.C. Elliott, *Structure and Chemistry of the Apatites and Other Calcium Orthophosphates. Studies in Inorganic Chemistry*, vol. 18, Elsevier, Amsterdam/London, 1994.
- [36] Z. Amjad, *Calcium Phosphates in Biological and Industrial Systems*, Kluwer Academic Publishers, Boston, MA, 1997.
- [37] S.V. Dorozhkin, *Comments Inorg. Chem.* 20 (1999) 285.
- [38] J.D. Bierlein, C.B. Arweiler, *Appl. Phys. Lett.* 49, 917, 1986.
- [39] J.D. Bierlein, A. Ferretti, L.H. Brixner, W.Y. Hsu, *Appl. Phys. Lett.* 50, 1216, 1987.
- [40] J.A. Wilder, *J. Non-Cryst. Solids* 38–39, 879, 1980.
- [41] B.C. Sales, *Mater. Res. Soc. Bull.* 12, 32, 1987.
- [42] J.J. Videau and V. Dupuis, *Eur. J. Solid State Inorg. Chem.* 28, 303, 1991.
- [43] A. Naeem, S. Mustafa, N. Rehana, B. Dilara and S. Murtaza, *J. of Colloid and Interface Sci.*, 252, 6-14, 2002.
- [44] F. Liebau, *Structural Chemistry of Silicates*, Springer Verlag, Heidelberg, 1985.
- [45] R. Kniep, H. Engelhardt, C. Hauf, *Chem. Mater.*, 10, 2930, 1998 and additional references therein.
- [46] R. Kniep, G. Schäfer, H. Engelhardt, I. Boy, *Angew. Int. Ed.*, 38, 3642, 1999. [47] A. K. Cheetham, G. Férey, T. Loiseau, *Angew. Int. Ed.*, 38, 3268, 1999.
- [48] R. P. Bontchev, J. Do, A. J. Jacobson, *Angew. Int. Ed.*, 38, 1937, 1999.
- [49] A. F. Wells, *Structural Inorganic Chemistry*, 4th ed., p. 851. Oxford, 1975.
- [50] R. J. Bell and A. Carnevale, *Philos. Mag.*, B 43(3), 389, 1981.
- [51] J. S. Ysker, R. Bohlho, H. Bambauer, and W. Hoffmann, *Z. Kristallogr.* 132, 457, 1970.
- [52] A. Rulmont and M. Almou, *Spectrochim. Acta Part A* 45(5), 603, 1989.
- [53] V. V. Krasnikov, Z. A. Konstant, and V. K. Belskii, *Neorg. Mater.*, 21, 1560, 1985.

- [54] A. Levesseur, R. Olazcuaga, M. Kbala, M. Zahir, P. Hagenmuller, and M. Couzi, *Solid State Ionics*, 2, 205, 1981.
- [55] H. Bauer, *Z. Anorg. Allg. Chemie.*, 345, 225, 1966.
- [56] (a) R. Tartarelli, M. Giorgini, A. Lucchesi, G. Stoppato, F. Moreli, *J. Catal.*, 17, 41, 1970;
- (b) J. Haber, U. Szybalska, *Faraday Discuss. Chem. Soc.*, 72, 263, 1981;
- (c) J.B. Moffat, *Catal. Rev. Sci. Eng.*, 18, 199, 1978;
- (d) S.S. Jewur, J.B. Moffat, *J. Catal.*, 57, 167, 1979;
- (e) J.B. Moffat, A. Schemidtmeyer, *Appl. Catal.*, 28, 161, 1986;
- (f) A. Tada, H. Suzuka, Y. Imizu, *Chem. Lett.*, 182, 423, 1987.
- [57] R. Kniep, H. Engelhard, C. Hauf, *Chem. Mater.*, 10, 2930, 1998.
- [58] R. P. Bontchev, J. Do, A. J. Jacobson, *Inorg. Chem.*, 38, 2231, 1999.
- [59] D. Mazza, S. Ronchetti, A. Dalmestro, M. Tribaudino and W. Kockelmann, *Chem. Mater.*, 2000.
- [60] R. Kniep, D. Koch, H. Borrmann, *New Crystal Structures* 217(2), 187-188, 2002.
- [61] R. Kniep, D. Koch, Th. Hartmann, *New Crystal Structures* 217(2), 186, 2002.
- [62] K. Goetzmann, K. Dorn, H. D. Naegerl, A. Espenschied, A. Klein, *Chemische Fabrik Budenheim Rudolf A. Oetker, Germany. Ger. Offen.* (1997), 7 pp. CODEN: GWXXBX DE 19525341 A1 19970116 Patent written in German.
- [63] Y. Shi, J. Liang, H. Zang, Q. Liu, X. Chen, J. Yang, W. Zhuang and G. Rao, *Crystal Structure and Thermal Decomposition studies of Barium Borophosphate, BaBPO₅*, *J. Solid State Chemistry* 135, 43-51, 1998.
- [64] A. Karthikeyani and R. Jagannathan, *J. Lumin.*, 86, 79, 2000.
- [65] G. Blasse, G. J. Dirksen and A. Meijerink, *Chem. Phys. Lett.*, 167, 41, 1990.
- [66] Q. Zeng, N. Kilah and M. Riley, *The luminescence of Sm²⁺ in alkaline earth borophosphates*, *J. of Luminescence*, 101, 167-174, 2003.
- [67] M. Scagliotti, M. Villa and G. Chiodelli, *J. Non-Cryst. Solids*, 93, 350, 1987.
- [68] M. Scagliotti, M. Villa and G. Chiodelli, *J. Non-Cryst. Solids*, 94, 101, 1987.
- [69] D. G. Grossmann and C. J. Philips, *J. Am. Ceram. Soc.*, 47, 471, 1964.
- [70] J. M. Clinton and W. W. Coffeen, *Ceram. Bull.*, 63, 1401, 1984.
- [71] Terran Technologies, Inc., 1995,1996,1997,1998.

- [72] R. Le Parc, B. Champagnon, J. Dianoux, P. Larry and V. Martinez, *J. of Non-Crys. Solids*, 323, 155-161, 2003.
- [73] Borg and Smith, *Am. Mineral*, 53, 1709, 1968.
- [74] Q. Yang, Y. Li, Q. Yin, P. Wang and Yi-Bing Cheng, Hydrothermal synthesis of bismuth oxide needles, *Materials Letters*, 55, 46-49, 2002.
- [75] S. H. Feng and R. R. Xu, *Acc. Chem. Res.*, 34, 239, 2001.
- [76] Seung-Beom Choa, Jun-Seok Noh, Malgorzata M. Lencka and Richard E. Riman., *Journal of the European Ceramic Society*, 23, 2323-2335, 2003.
- [77] A. Stein, S. W. Keller, and T. E. Mallouk, *Science* 259, 1558, 1993., X.-Q. Xin, and L.-M. Zheng, *J. Solid State Chem.* 106, 451, 1993.
- [78] X.-Q. Xin, and L.-M. Zheng, *J. Solid State Chem.* 106, 451, 1993.
- [79] R. B. Schwarz, and W. L. Johnson, *Phys. Rev. A*, 51, 415, 1983., B. X. Liu, O. Jin, and Y. Ye, *J. Phys.: Cond. Matter.*, 8, L79, 1996.
- [80] L. Qingwen, W. Yiming, L. Guoan, *Sensors Actuators B* 59, 42, 1999.
- [81] D. M. Thomas and E. M. McCarron, III, *Mater. Res. Bull.*, 21, 945, 1986.
- [82] Q. He, X. Yang, H. Guo, Y. Yuan and H. Li, *Materials Letters*, 57, 3609 - 3613, 2003.
- [83] A. Uztetik-Amour and M. Kızılyallı, *High Temperature and Materials Science*, 36, 77-85, 1996.
- [84] A. Uztetik, PhD Thesis, Middle East Technical University Ankara, Turkey, 1992.
- [85] M. T. Averbuch-Pouchot and A. Durif, *Acta Cryst.*, C 43, 631-632, 1986.
- [86] J. Bennazha, A. Boukhari and E. M. Holt, *Acta. Cryst. C* 58, 129-130, 2002.
- [87] M. Rokita, M. Handke and W. Mozgawa, *J. Molecular Structure*, 555, 351-356, 2000.
- [88] E. Görlich, *The Effective Nuclear Charges and Electronegativity*, PAN Krakov, 1997.

APPENDIX A

Table A. The X-ray Powder Diffraction Data of BPO₄ (J.C.P.D.S. Card. No: 34-132)

I/I₀	d(Å)	hkl
100	3.6351	101
3	3.3207	002
4	3.0699	110
34	2.2546	112
2	1.9719	103
10	1.8641	211
5	1.8175	202
<1	1.6604	004
1	1.5354	220
10	1.4597	213
<1	1.4146	301
<1	1.3936	222
2	1.3732	310
5	1.3192	204
4	1.2689	312
2	1.2114	303
4	1.1851	321
1	1.1272	224
<1	1.1069	006
2	1.0964	215
<1	1.0859	400
1	1.0580	314, 323
3	1.0402	411
<1	1.0319	402
<1	0.9862	206
1	0.9781	332

APPENDIX B

Table B. The X-ray Powder Diffraction Data of $\text{AlPO}_4 \cdot x\text{H}_2\text{O}$ (J.C.P.D.S. Card. No: 15-265)

I/I_0	$d(\text{\AA})$
7.280	40
4.900	60
4.580	30
4.360	20
3.920	100
3.690	80
3.450	40
3.390	40
3.190	30
3.110	20
2.995	40
2.860	60
2.794	10
2.758	50
2.708	5
2.648	10
2.511	60
2.501	20
2.452	30
2.423	10
2.251	30

APPENDIX C

Table C. The X-ray Powder Diffraction Data of $\text{Al}(\text{PO}_3)_3$ (J.C.P.D.S. Card. No: 13-0264)

I/I_0	$d(\text{Å})$
50	5.340
60	5.150
50	4.560
100	3.803
70	3.694
70	3.604
10	3.450
10	3.430
100	3.346
60	3.194
50	3.116
70	3.010
30	2.978
20	2.952

APPENDIX D

Table D. The X-ray Powder Diffraction Data of AlPO_4 (J.C.P.D.S. Card. No: 47-0712)

I/I_0	$d(\text{\AA})$
20	9.300
100	6.660
2	6.230
2	6.030
12	5.640
39	4.900
32	4.820
16	4.430
11	4.270
1	4.200
3	4.000
2	3.900
12	3.680
13	3.620
4	3.510
39	3.350
21	3.080
11	3.020
21	2.960
43	2.800